Weierstraß-Institut
für Angewandte Analysis und Stochastik

Leibniz-Institut im Forschungsverbund Berlin e. V.

Preprint ISSN 2198-5855

A hybrid FETI-DP method for non-smooth random partial differential equations

Martin Eigel, Robert Gruhlke

submitted: December 21, 2018 (revision: August 23, 2019)

Weierstrass Institute
Mohrenstr. 39
10117 Berlin
Germany
E-Mail: martin.eigel@wias-berlin.de
robert.gruhlke@wias-berlin.de

No. 2565
Berlin 2018

2010 *Mathematics Subject Classification.* 35R60, 47B80, 60H35, 65C20, 65N12, 65N22, 65N55, 65J10 .

Key words and phrases. Elliptic pde, partial differential equations with random coefficients, domain decomposition, FETI, non-smooth, uncertainty quantification, stochastic finite element method .

Edited by
Weierstraß-Institut für Angewandte Analysis und Stochastik (WIAS)
Leibniz-Institut im Forschungsverbund Berlin e. V.
Mohrenstraße 39
10117 Berlin
Germany

Fax: +49 30 20372-303
E-Mail: preprint@wias-berlin.de
World Wide Web: http://www.wias-berlin.de/

A hybrid FETI-DP method for non-smooth random partial differential equations

Martin Eigel, Robert Gruhlke

ABSTRACT. A domain decomposition approach for high-dimensional random PDEs exploiting the localization of random parameters is presented. To obtain high efficiency, surrogate models in multi-element representations in the parameter space are constructed locally when possible. The method makes use of a stochastic Galerkin FETI-DP formulation of the underlying problem with localized representations of involved input random fields. The local parameter space associated to a subdomain is explored by a subdivision into regions where either the parametric surrogate accuracy can be trusted or where instead Monte Carlo sampling has to be employed, which is the case for a non-smooth parameter dependence. A heuristic adaptive algorithm carries out a problem-dependent hp refinement in a stochastic multi-element sense, anisotropically enlarging the trusted surrogate region in local parametric space as far as possible. This results in an efficient global parameter to solution sampling scheme making use of local parametric smoothness exploration in the involved surrogate construction. Adequately structured problems for this scheme occur naturally when uncertainties are defined on sub-domains, e.g. in a multi-physics setting, or when the Karhunen-Loève expansion of a random field can be localized. The efficiency of the proposed hybrid technique is assessed with numerical benchmark problems illustrating the identification of trusted (possibly higher order) surrogate regions and non-trusted sampling regions.

1. INTRODUCTION

In Uncertainty Quantification (UQ), numerical methods typically are either based on pointwise sampling, which is applicable to quite general problems but rather inefficient, or they rely on (an often analytic) smoothness of the parameter to solution map with the parameters determining the randomness. However, in many science and engineering applications deviating from the common Darcy benchmark setting with smooth Karhunen-Loève random fields, higher smoothness cannot be assumed globally in the parameter domain and physical space. This severely limits the use of techiques relying on sparsity or low-rank approximability.

As a prototypical application example, which is for instance of relevance in material science, we have in mind a *composite material with random non-periodic inclusions*. This setting exhibits discontinuities in the parameter dependence, rendering it basically intractable to functional approximations with global basis functions in parameter space as commonly used in Stochastic Galerkin FEM, Stochastic Collocation and other non-intrusive projection approaches.

While Monte Carlo sampling and its modern variants (e.g. Multilevel and Quasi Monte Carlo, [9], [34]) are widely applicable and robust, smoothness can only be used to a limited extend, resulting in slow convergence in the number of samples. Nevertheless, for problems with low parameter regularity, a sampling approach might seem the only option to pursue. It is a central aim of this work to overcome this restriction as beneficial as possible. Sampling approaches have been analysed for random material coefficients spatially being piecewise continuous in [45] or essentially bounded in [6]. In both references the approximation of the material coefficients itself, *e.g.* through the discretization process was eschewed, leaving out the effect of discontinuities not being resolved perfectly, see example 2.8 and 2.9. Within the first part of this paper we attemp to close this gap while relying on weaker spatial norms begin of L^p, $p < \infty$ type instead of $p = \infty$ as in [6].

A notion not frequently used for this kind of problems is a localization of randomness, *e.g.* by means of a domain decomposition method, as employed here. In fact, the guiding principle is to make the high-dimensional problem more accessible by considering smaller physical domains, locally leading to a dependence on fewer relevant random variables. However, since the local representations cannot be assumed independent from each other, a weak coupling condition has to be introduced. To achieve

DOI 10.20347/WIAS.PREPRINT.2565 Berlin, December 21, 2018/rev. August 2019

this, we rely on the well-known theory of domain decomposition techniques and in particular the class of FETI and FETI-DP methods, see e.g. [32, 31, 30]. These methods were also investigated for random problems *e.g.* in [43, 11, 25]. For more details and references, we refer to Section 4. To develop these approaches further, we introduce the concept of *trust* and *no-trust regions* for a prescribed error tolerance [25] locally in which the highly efficient surrogate can be evaluated ("trusted") or where one has to fall back to standard pointwise sampling ("non-trusted"). Local surrogates can be generated in parallel and depend only on local random coordinates. In order to get the largest gain from the construction, trust regions are required to cover an area of the parameter domain related to each subdomain as large as possible. For this, we introduce a *local generalized multi-element discretization* in the local parameter spaces, for which an hp adaptive refinement procedure based on error indicators is presented.

The proposed hybrid stochastic FETI-DP allows for fast global sampling on the basis of *local smoothness exploitation* by appropriate surrogates.

The paper is structured as follows: The next section introduces the considered linear random model problem and provides an overview of the perturbation and convergence theory in particular for the case motivating this work, namely non-smooth coefficients. Section 3 examines the construction of surrogate models, which are used locally in the method. Special attention is paid to generalized multi-element polynomial chaos expansions and a partition of unity interpolation. The employed parametric domain decomposition method is derived in Section 4, which leads to a parametric FETI-DP method pivotal in our approach. Eventually, Section 5 demonstrates the accuracy and adaptive refinement behaviour of the hybrid sampling approach with some benchmark problems.

2. Model problem and a-priori estimates

In this section, we introduce the random linear elliptic model problem used henceforth for the derivation of the proposed domain decomposition method. Of particular interest is the effect of approximation errors of the coefficient, which is of particular relevance for simulations with random data models. We examine conditions required for stability results of the approximate solution, especially in the case of non-smooth coefficients. A prototypical application we have in mind is the numerical treatment of *stochastic composite materials*. This type of problem is much more involved than the frequently considered case of random PDEs with smooth data in Uncertainty Quantifications as *e.g.* presented in [2, 3, 13, 16, 17], where the dependence on the countable (possibly infinite) parameter vector is analytic. Such a smooth dependence allows for the derivation of best n-term approximations with optimal (exponential) convergence rates and, while still computationally costly, the implementation of efficient numerical methods, respectively.

For the reader mainly interested in the algorithmic aspects of the proposed hyprid sampling approach, we suggest to only skim through this section to understand the examined model problem and the structure of the considered non-smooth problems by the examples provided at the end.

2.1. Random PDE Model.

As model problem we consider a random linear partial differential equation (PDE). Given a probability space $(\Omega, \mathcal{U}, \mathbb{P})$, a Lipschitz domain $D \subset \mathbb{R}^d$ for $d = 2, 3$, with Dirchlet and Neumann boundary segments $\Gamma_0, \Gamma_1 \subset \partial D$, s.t. $\partial D = \Gamma_0 \cup \Gamma_1$, $\Gamma_1 \cap \Gamma_0 = \emptyset$ and $|\Gamma_0| > 0$. Then, the stationary diffusion model equation reads pointwise for $\omega \in \Omega$ a.e.

$$\left\{ \begin{array}{rcll} -\operatorname{div}\left(A(x,\omega)\nabla u(x,\omega)\right) &=& f(x,\omega) & \text{in } D, \\ \mathbf{n}^T A(x,\omega)\nabla u(x,\omega) &=& g(x,\omega) & \text{on } \Gamma_1, \\ u(x,\omega) &=& 0 & \text{on } \Gamma_0. \end{array} \right. \tag{1}$$

Here A denoted the diffusion field, f and g are source fields and $\boldsymbol{n}$ is the outer normal on Γ_1 w.r.t. D. In the following, we state pathwise and global assumptions in the setting of elliptic (pathwise) second

order PDEs. In the context of integrability, we use lower case letters for spatial integrability and upper case letters for stochastic integrability, *e.g.* $L^p(D)$ or $L^P(\Omega)$.

(*PA1*) For a.e. $x \in D$, $\omega \in \Omega$, the $d \times d$ matrix $A(x,\omega)$ is symmetric and positive definite. Denote by $\lambda_{\text{min/max}}(A(x,\omega))$ the smallest and largest eigenvalues of $A(x,\omega)$ and define

$$\lambda_{\text{min}}(A(.,\omega)) := \operatorname*{ess\,inf}_{x\in D} \lambda_{\text{min}}(A(x,\omega)),$$
$$\lambda_{\text{max}}(A(.,\omega)) := \operatorname*{ess\,sup}_{x\in D} \lambda_{\text{max}}(A(x,\omega)).$$

Then there exist $\underline{c}, \overline{c}\colon \Omega \to \mathbb{R}$ such that there hold pathwise uniform bounds a.e. in ω,

$$0 < \underline{c}(\omega) \le \lambda_{\text{min}}(A(.,\omega)) \le \lambda_{\text{max}}(A(.,\omega)) \le \overline{c}(\omega) < \infty. \tag{2}$$

(*PA2*) The random variable $\underline{c}(\omega)^{-1}$ is an element of $L^R(\Omega)$ for some $R \in [1,\infty]$.

(*A1*) There exists $c > 0$ such that $0 < c < \underline{c}(\omega)/\overline{c}(\omega) \le 1$, a.e. in Ω.
(*A2*) Uniform bounds: $0 < \underline{C}, \overline{C} < \infty$ such that $\operatorname{ess\,inf} \underline{c}(\omega) \ge \underline{C}$ and $\operatorname{ess\,sup} \overline{c}(\omega) \le \overline{C}$.
(*A3*) It holds $g \in L^P(\Omega; H_{00}^{-1/2}(\Gamma_1))$ and $f \in L^P(\Omega; (H^1_{\Gamma_0})^*)$ for some $P \in [1,\infty]$ (cf. [42]).

Remark 2.1. *Note that the uniform bound assumption (A2) is not necessary for pathwise existence and uniqueness of a weak solution. However, it turns out to be useful for interpolation arguments employed later and the p-condition with $p \neq p(\omega)$.*

We define the pathwise bilinear form a associated to the weak formulation of (1) for a given diffusion field B satisfying pathwise assumptions (*PA1*)–(*PA2*) as

$$a[B,\omega](w,v) := \int_D B(x,\omega)\nabla w(x)\cdot\nabla v(x)\,\mathrm{d}x, \quad \forall w,v \in H^1_{\Gamma_0}(D),$$

and the pathwise linear form

$$\ell[\omega](v) := \int_D f(x,\omega)v(x)\,\mathrm{d}x + \int_{\Gamma_{\text{N}}} g(\omega,x)v(x)\,\mathrm{d}s, \quad \forall v \in H^1_{\Gamma_0}(D).$$

Then the pathwise weak formulation given B for $\omega \in \Omega$ reads

$$\text{Seek } u(\omega) \in H^1_{\Gamma_0}(D) \text{ s.t. } a[B,\omega](u(\omega),v) = \ell[\omega](v), \quad \forall v \in H^1_{\Gamma_0}(D). \tag{3}$$

Lemma 2.2. *(cp.* [6]*) Let assumptions (PA1)–(PA2) and (A3) hold with $S = (1/P + 1/R)^{-1} \ge 1$. Then there exists a unique pathwise weak solution $u(\omega) \in H^1_{\Gamma_0}(D)$ of* (3) *with $B = A$ for $\mathbb{P}$-almost all $\omega \in \Omega$ with $u \in L^S\left(\Omega; H^1_{\Gamma_0}\right)$.*

2.2. **Error estimate for coefficient approximate solutions.** Let $\hat{A}$ be some pertubation of A in (1), *e.g.* implicitly introduced by a quadrature or triangulation scheme in the discretization process. Let u and $\hat{u}$ be (pointwise) weak solutions with respect to A and $\hat{A}$. Then, we are interested in the distance of u to $\hat{u}$ in the abstract sense of

$$u \to \hat{u} \quad \text{if} \quad A \to \hat{A}, \tag{4}$$

where the type of convergence has to be determined.

2.2.1. *Pathwise error estimates.* Let $u(\omega)$ be the solution of (3) with $B = A$ and let $\hat{u}(\omega)$ be the solution of (3) with $B = \hat{A}$. Denote by $\underline{\hat{c}}\colon \Omega \to \mathbb{R}$ the lower bound random variable with respect to $\hat{A}$ satisfying assumptions (*PA1*)–(*PA2*). For simplicity, we shall assume that the right-hand side linear form can be evaluated exactly. Then it holds

$$a[A,\omega](u(\omega),v(\omega)) = a[\hat{A},\omega](\hat{u}(\omega),v(\omega)). \tag{5}$$

Inserting $0 = \hat{A}(x,\omega)\nabla u(x) - \hat{A}(x,\omega)\nabla u(x,\omega)$, one obtains

$$a[\hat{A},\omega](u(\omega)-\hat{u}(\omega),v(\omega)) = a[A-\hat{A},\omega](u(\omega),v(\omega)). \tag{6}$$

Now taking $v = u - \hat{u}$ and due to the assumptions on A, the left-hand side can be estimated from below by

$$\underline{\hat{c}}(\omega)\|u(\omega)-\hat{u}(\omega)\|^2_{H^1_{\Gamma_0}} \leq \left| a[\hat{A},\omega](u(\omega)-\hat{u}(\omega),u(\omega)-\hat{u}(\omega)) \right|. \tag{7}$$

Let us assume that $\nabla u(\omega)$ is in $L^p(D)$ for some $p \geq 2$. Then for q such that $1/p + 1/q = 1$, $q = 2p/(2-p) \in [2,\infty]$, we obtain pathwise

$$\left| a[A-\hat{A},\omega](u(\omega),v(\omega)) \right| \leq \|A(.,\omega)-\hat{A}(.,\omega)\|_{L^q(D)}\|\nabla u(\omega)\|_{L^p(D)}\|\nabla v(\omega)\|_{L^2(D)}. \tag{8}$$

Combining (7) and (8) yields

$$\|u(\omega)-\hat{u}(\omega)\|_{H^1_{\Gamma_0}(D)} \leq \underline{\hat{c}}(\omega)^{-1}\|A(.,\omega)-\hat{A}(.,\omega)\|_{L^q(D)}\|\nabla u(\omega)\|_{L^p(D)}. \tag{9}$$

Based on this derivation, we can refine the above statement to a decomposition of the spatial domain D with relaxed integrability requirements of ∇u in each subdomain.

Lemma 2.3. *(**local perturbation**) Let $\overline{D} = \overline{\cup_{s=1}^{N_{SD}} D_s}$ with piecewise disjoint subdomains $\{D_s\}_{s=1}^{N_{SD}}$. For $s = 1,\dots,N_{SD}$, assume that $[\nabla u]_{|D_s}(\omega) \in L^{p_s}(D_s)$ for $p_s \geq 2$ and a.e. $\omega \in \Omega$ and let $q_s = 2p_s/(p_s-2)$. Then,*

$$\|u(\omega)-\hat{u}(\omega)\|_{H^1_{\Gamma_0}(D)} \leq \underline{\hat{c}}(\omega)^{-1}\left[\sum_{s=1}^{S}\|\nabla u(\omega)\|_{L^{p_s}(D_s)}\|A(\omega)-\hat{A}(\omega)\|_{L^{q_s}(D_s)}\right]. \tag{10}$$

For $p_s = 2$ for $s = 1,\dots,N_{\mathrm{SD}}$, the perturbation result recovers the standard L^∞ estimate, w.r.t. A. We are left with the question of integrability of ∇u. Here, we state a pathwise $p*$-condition motivated by [7] in our random framework.

Definition 2.4. *(p^***-condition**)*
Let an integrability constant $p^* = p^*(A,d,D) > 2$ be independent of ω and let $2 \leq p < p^*$. Additional if $|\Gamma_1| > 0$ there is a conormal derivative trace space $X^p(\Gamma_1) := X(p,\Gamma_1,\Gamma_0)$ with $g(\omega) \in X^p$. Furthermore, for $f(\omega) \in W^{1,p}_{\Gamma_0}(D)^*$ and $u(\omega) \in W^{1,p}_{\Gamma_0}(D)$ and a random variable $C_p(\omega) = C_p(d,A,D)(\omega)$ the following estimate holds true

$$\|\nabla u(\omega)\|_{L^p(D)} \leq C_p(\omega)\left(\|f(\omega)\|_{W^{1,p}_{\Gamma_0}(D)^*} + \|g(\omega)\|_{X^p(\Gamma_1)}\right), \quad \omega \in \Omega. \tag{11}$$

Here, $X^p(\Gamma_1) \subset W^{-\frac{1}{p},p}(\Gamma_1)$ is a closed subspace with equality if $\Gamma_0 = \emptyset$ respecting DIRICHLET data in the spirit of the LIONS-MAGENES space $H^{-1/2}_{00}(\Gamma_1)$ [44] obtained by interpolation [47] as the dual of the space $[W^{1,p'}_0, L^{p'}]_{1/p,p}$ with $1/p + 1/p' = 1$ defined on the NEUMANN boundary segment.

We emphasize the most common setting with $p = 2$ and $q = \infty$. In this HILBERTian case, $C_2(\omega) = \underline{c}(\omega)^{-1}C(D,\Gamma_0)$ with $\underline{c}$ from Assumption (*PA1*) and a deterministic constant $C(D,\Gamma_0)$ determined by POINCARÉ and trace inequality constants.

For $p > 2$, the verification of this condition is somewhat more involved but fortunately still holds true. In the case of a purely homogeneous DIRICHLET boundary, *i.e.* $|\Gamma_1| = 0$ and for the plain LAPLACIAN

with $A \equiv I$, for any LIPSCHITZ domain it follows by [29] that there exist $\overline{p}^* = \overline{p}^*(d, D) > 3$ ($\overline{p}^* > 4$ for $d = 2$) and a constant $K = K(\overline{p}^*, D)$ such that for all $2 \leq p \leq \overline{p}^*$,

$$\|\nabla u(\omega)\|_{L^p(D)} \leq K \|f(\omega)\|_{W^{1,p}_{\Gamma_0}(D)^*}. \tag{12}$$

The result extends to $A(\omega) \neq I$ by a perturbation argument (see [36, 7]) and can in particular be translated to our pathwise framework. Define

$$p^*\colon (0,1) \to (2, \overline{p}^*), \qquad p^*(t) := \operatorname{argmax}\{K^{-\eta(p)} > 1 - t\colon 2 < p < \overline{p}^*\} \tag{13}$$

with $\eta(p) := (1 - 2/p)/(1 - 2/\overline{p}^*) \in (0, 1)$ monotonously increasing. With this construction, there are random variables

$$\overline{p}^*(\omega) := p^*(\underline{c}(\omega)/\overline{c}(\omega)), \quad C_p(\omega) := \frac{1}{\overline{c}(\omega)} \frac{K^{\eta(p)}}{1 - K^{\eta(p)}(1 - \underline{c}(\omega)/\overline{c}(\omega))}, \tag{14}$$

depending on the random variable bounds $\underline{c}, \overline{c}$ of A from (*PA1*). An important observation is that $p^*(t)$ is monotonously decreasing in t. With this construction in mind, let $u(\omega)$ be the pathwise solution of (3) with $B = A$ satisfying Assumption (*PA1*). Then for $2 \leq p < p^*(\underline{c}(\omega)/\overline{c}(\omega))$ pathwise, a.e. it holds

$$\|\nabla u(\omega)\|_{L^p(D)} \leq C_p(\omega) \|f(\omega)\|_{W^{1,p}_{\Gamma_0}(D)^*}. \tag{15}$$

Hence, in order to satisfy the p^*-condition in Definition 2.4, the quotient $\underline{c}(\omega)/\overline{c}(\omega)$ needs to be bounded away from zero to obtain $\operatorname{ess\,inf} \overline{p}^*(\omega) > 2$, which motivates Assumption (*A1*). This result is summarized in the following theorem.

Theorem 2.5. *Assume $|\Gamma_1| = \emptyset$. Let $f(\omega) \in W^{-1,p}(D)$ and $u(\omega) \in W^{1,p}_0(D)$ the corresponding solution of* (3) *with $B = A$ satisfying (PA1), (PA2) and (A1) with $2 \leq p < p^* := p^*(c)$ for $c > 0$ from (A1). Then the p^*-condition holds true.*

Note that the uniform boundedness Assumption (*A2*) implies (*A1*). The case of mixed boundary conditions and L^p estimates of solution gradients can be derived from results of [24]. $W^{1,p}(D)$ estimates for ROBIN boundary conditions can be obtained from [1] with boundary right-hand side in $W^{-\frac{1}{p},p}(\partial D)$.

We end the pathwise discussion of this section with an examination of the (p, q) relation. There are two important cases:

1 $q = \infty$, thus $p = 2$: In order to have pathwise $\hat{u}(\omega) \to u(\omega)$ in $H^1_{\Gamma_D}(D)$, we necessary need that $\hat{A}(\omega) \to A(\omega)$ in $L^\infty(D)^{d,d}$. This situation applies in case of
   - *higher regularity*: $A(\cdot, \omega) \in C^{k,\alpha}(D)$ yields an error of at least $\mathcal{O}(h^k)$ using an appropriate quadrature scheme.
   - *exact meshing*: $A(., \omega)$ is only piecewise $\mathcal{C}^{k,\alpha}$ with (a-priori known, *e.g.* [45]) discontinuities exactly being resolved, e.g. through adapted meshes with possible curved cells

2 $q < \infty$, thus $p > 2$: This case is important if $A(\cdot, \omega)$ *lacks spatial regularity or cannot be resolved in a discretisation step* by some $\hat{A}$ such that the error in the L^∞ norm stays $\mathcal{O}(1)$. In this case, the $q = \infty, p = 2$ estimate might become meaningless. However, the p^*-condition still ensures convergence of the perturbed solution based on weaker approximation requirements on the coefficient. At this point, one may ask for the approximation in the weakest norm possible, that is $q = 2$ such that

$$\|A(\omega) - \hat{A}(\omega)\|_{L^2(D)^{d,d}} \to 0 \quad \Rightarrow \quad \|u(\omega) - \hat{u}(\omega)\|_{H^1_{\Gamma_0}(D)} \to 0. \tag{16}$$

   We note that this indeed is possible by an interpolation argument, assuming that A and $\hat{A}$ satisfy the uniform boundedness (*PA1*) and (*A2*). Then,

$$\|A(\omega) - \hat{A}(\omega)\|_{L^q(D)^{d,d}} \leq C(q) \|A(\omega) - \hat{A}(\omega)\|^{1/q}_{L^2(D)^{d,d}}, \tag{17}$$

with a constant $C(q) = C(q, \|A - \hat{A}\|_{L^\infty})$. Since $\hat{A}(\omega)$ and $A(\omega)$ are assumed to be in $L^\infty(D)^{d,d}$, we obtain by interpolation that

$$\|A(\omega) - \hat{A}(\omega)\|_{L^q(D)^{d,d}} \leq C(q)\|A(\omega) - \hat{A}(\omega)\|^{1/q}_{L^2(D)^{d,d}}. \tag{18}$$

As a consequence, in order to obtain a pathwise good approximation $\hat{u}(\omega)$ of $u(\omega)$, it is sufficient to control the L^2 approximation $\hat{A}(.,\omega)$ of $A(.,\omega)$. However, we note that by the employed interpolation this estimate introduces a reduced convergence order by a factor $1/q$. Hence, ideally one can strive for an L^q approximation to avoid a degeneration of the convergence order.

2.2.2. *Global error estimates.* We now analyse how the distance of $\hat{A}$ to A transfers to the approximation of the solution $\hat{u}$ to u. More specifically, we are interested in an estimate of the form $\|u - \hat{u}\|_1 \leq h(\|A - \hat{A}\|_2)$, with continuous $h : \mathbb{R}^+ \to \mathbb{R}^+$, $h(0) = 0$ and suitable norms $\|.\|_1$ and $\|.\|_2$ such that $u \to \hat{u}$ in $\|\cdot\|_1$ if $\hat{A} \to A$ in $\|\cdot\|_2$. We state the main result of this subsection.

Theorem 2.6. ***(A-priori $L^q(D)$-perturbation estimate)***
Let $P, Q, R_1, R_2 \in [1,\infty]$, such that $S := (1/P + 1/Q + 1/R_1 + 1/R_2)^{-1} \geq 1$ and let the p^*-condition of Definition 2.4 hold. For $2 \leq p < p^*$, assume $C_p(\cdot) \in L^{R_2}(\Omega)$ and let $f \in L^P(\Omega; W^{1,p}_{\Gamma_0}(D)^*)$ and $g \in L^P(\Omega; X^p_{\Gamma_1})$. Let $u(\omega)$ and $\hat{u}(\omega)$ be the unique solution from (3)*, with $B = A($ and $B = \hat{A}$, respectively, satisfying assumptions (PA1)–(PA2) with $R = R_1$. If $A, \hat{A} \in L^Q(\Omega; L^q(D))$ for $q = 2p/(2-p)$ such that $\hat{A}$ satisfies (PA1) with lower bound $\underline{\hat{c}}(\cdot)^{-1} \in L^{R_1}(\Omega)$, then*

$$\|u - \hat{u}\|_{L^S(\Omega; H^1_{\Gamma_0}(D))} \leq C\|A - \hat{A}\|_{L^Q(\Omega; L^q(D))}, \tag{19}$$

with $C = C(C_p, \underline{\hat{c}}, f, g)$.

Proof. By (9) and the p^*-condition, it holds pathwise that

$$\begin{aligned}\|u(\omega) - \hat{u}(\omega)\|_{H^1_{\Gamma_0}} &\leq \underline{\hat{c}}(\omega)^{-1}\|A(\omega) - \hat{A}(\omega)\|_{L^q(D)}\|\nabla u(\omega)\|_{L^p(D)} \\ &\leq \underline{\hat{c}}(\omega)^{-1} C_p(\omega)\|A(\omega) - \hat{A}(\omega)\|_{L^q(D)} \\ &\quad \times \left(\|f(\omega)\|_{W^{1,p}_{\Gamma_0}(D)^*} + \|g(\omega)\|_{X^p(\Gamma_1)}\right).\end{aligned}$$

The result then follows by multiple applications of the HÖLDER inequality. Choose α such that $Q = \alpha T$ and denote by α' its conjugate exponent. Then, skipping the pathwise dependence, this yields

$$\begin{aligned}\|u - \hat{u}\|^T_{L^T(\Omega, H^1_{\Gamma_0}(D))} &\leq \left\| \underline{\hat{c}}^{-1} C_p \|A - \hat{A}\|_{L^q(D)} \right\|^T_{L^{T\alpha'}(\Omega)} \\ &\quad \times \left\| (\|f\|_{W^{1,p}_{\Gamma_0}(D)^*} + \|g\|_{X^p(\Gamma_1)}) \right\|^T_{L^Q(\Omega)}.\end{aligned}$$

Further iterative application of HÖLDER estimates yield the desired result. □

The a-priori perturbation estimation gives a qualitative statement of some closeness of the approximation to the true solution if the approximation error of the involved coefficient A is controlled. We point out that the important case of coefficients that are numerically approximated in $L^Q(\Omega, L^\infty)$ is included. However, note that in this case the need of a p^*-condition can be relaxed.

Corollary 2.7. ***(A-priori $L^\infty(D)$ perturbation estimate)***
Let $P, Q, R_1, R_2 \in [1,\infty]$ such that $S := (1/P + 1/Q + 1/R_1 + 1/R_2)^{-1} \geq 1$ and assume $f \in L^P(\Omega; H^1_{\Gamma_0}(D)^*)$ and $g \in L^P(\Omega; H^{-1/2}_{00}(\Gamma_1))$. Let $u(\omega)$ and $\hat{u}(\omega)$ be the unique solutions of

(3) *with* $B = A$ *and* $B = \hat{A}$ *satisfying assumptions (PA1) and (PA2) with* $R = R_1$ *and* $R = R_2$, *respectively. Then, for* $A, \hat{A} \in L^Q(\Omega; L^\infty(D))$ *it holds*

$$\|u - \hat{u}\|_{L^S(\Omega;H^1_{\Gamma_0}(D))} \leq C\|A - \hat{A}\|_{L^Q(\Omega;L^\infty(D))}. \tag{20}$$

While the assumptions in Corollary 2.7 are rather mild, the important case of random fields A representing *composite random materials with random inclusions* (to be examined in the following example) might nevertheless be excluded. If this type of materials is modeled pathwise by piecewise HÖLDER continuous or even smoother data then it fits in the setting of Theorem 2.6. We shall illustrate this line of thought with a small example.

Example 2.8. ***(Composite material)***
Consider $D = [-1, 1]^d$ *for* $d = 2, 3$ *and let* $\varrho \sim \mathcal{U}[0, R]$ *and* $R < \overline{R} < 1$ *such that*

$$\alpha(x, \omega) = \alpha(x, r(\omega)) = \kappa_1 \chi_{B_{\varrho(\omega)}(\mathbf{0})}(x) + \kappa_2(1 - \chi_{B_{\varrho(\omega)}(\mathbf{0})}(x))$$

with the EUCLID*ean centered ball of radius* $r(\omega)$ *denoted by* $B_{\mathbf{r}(\omega)}(\mathbf{0})$ *and an indicator function* χ, *see Figure 1. In mesh based discretization schemes using standard* GAUSSIAN *quadrature rules, the spherical random interfaces and thus the jump of the coefficient* $A(x, \omega) := \alpha(x, \omega)I$ *cannot be approximated pathwise in* $L^\infty(D)$. *In particular, for any such finite quadrature scheme, by the* GIBBS *phenomenon this error is* $\mathcal{O}(1)$ *with respect to the* L^∞ *norm.*

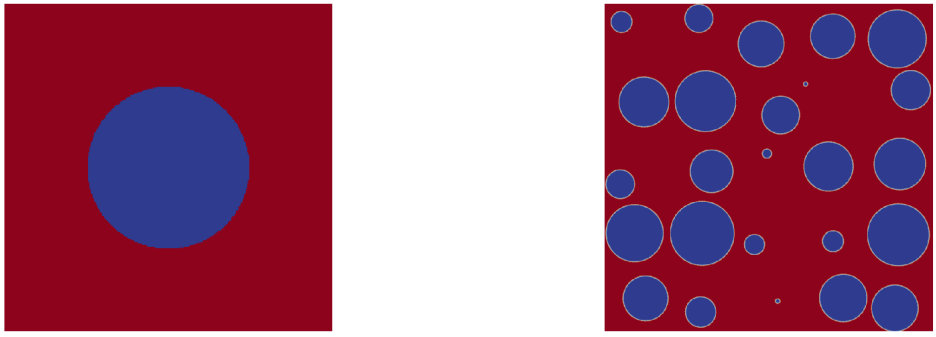

FIGURE 1. **Left**: Realization of composite material A from example 2.8; **Right**: Realization with multiple separated inclusions of example 2.9

Example 2.9. ***(Composite material approximation)***
Consider a partition of $D = [0, 1]^d$ *into disjoint squared subdomains* $\{D_s\}$ *with side length* $2R_s$. *Given the tensor parameter domain* $\Xi^r := [-1, 1]^{d+1}$, *enumerated by* $r = s$, *consider a bijective mapping* $\varphi^r : \Xi^r \to \mathcal{K}^r_\delta$ *for some* $0 < \delta \ll 1$ *with*

$$\mathbf{y}^r := (y^r_0, y^r_1, \ldots, y^r_d) \mapsto \varphi^r(\mathbf{y}^r) =: (\varrho, \mathbf{p}^r) = (\varrho, p^r_1, \ldots, p^r_d)$$

and $\mathcal{K}^r_\delta = \{(\varrho, \mathbf{p}^r) \in [0, R] \times D_s : \varrho < \operatorname{dist}(\mathbf{p}^r, \partial D_s) - \delta\}$ *for* $R > 0$. *Here* φ^r *maps the parameter* $\boldsymbol{y}^r$ *to a radius* ϱ *and a point* $\boldsymbol{p}^r$ *within* D_s *modeling variability in the size and the position of a circular inclusion having a positive distance* δ *from the boundary* ∂D_s. *Then with* $\boldsymbol{y} = (\boldsymbol{y}^r)_r$ *the mapping*

$$D \times \left(\bigtimes_{r=1}^{N_{SD}} \Xi^r\right) \ni (x, \mathbf{y}) \mapsto \alpha(x, \varphi(\mathbf{y})) = \sum_{s=1}^{N_{SD}} \chi_{D_s}(x) \left(\kappa_1 \chi_{B_\varrho(\mathbf{p}^s)}(x)) + \kappa_2(1 - \chi_{B_\varrho(\mathbf{p}^s)}(x))\right) \tag{21}$$

yields a parameteric representation of a composite material with inclusions defined on non-overlapping subdomains having variable positions and sizes, see Figure 1.

In a numeric simulation, we may approximate this setting *e.g.* by the following approaches

- $\hat{\alpha}_{MC}$ is a pathwise projection of $\alpha(\cdot, \mathbf{y})$ to piecewise constants on an underlying mesh,
- $\hat{\alpha}$ might be a cluster approximation, that is a piecewise constant approximation with respect to the parameter $\mathbf{y}$, see section 4.2.4
- $\hat{\alpha}$ is implicitly approximated when surrogates in domain decomposition methods (like parameter dependend local Schur complements) are approximated continuously by piecewise affine functions, see section 5.2.

All of the above approximation schemes are not converging in $L^Q(\Xi; L^\infty(D))$.

Remark 2.10. *The convergence assumption in $L^Q(\Omega; L^q(D))$ and the requirements of the p^* condition can be further relaxed in the fully discretized setting. In fact, it only has to hold*

$$U_\ell \subset U := L^2(\Omega; H^1_{\Gamma_0}(D)) \hookrightarrow H := L^2(\Omega, L^2(D)), \tag{22}$$

with discrete space U_ℓ with $\dim U_\ell < \infty$ on level $\ell \geq 0$. Let

$$b[B](u, v) := \int_\Omega \int_D B(x, \omega) \nabla u(x, \omega) \cdot \nabla v(x, \omega) \mathrm{d}x \mathrm{d}\mathbb{P}. \tag{23}$$

In the discrete case, by STRANG*'s Lemma, one needs an estimate of*

$$|b[A](w_\ell, v_\ell) - b[\hat{A}](w_\ell, v_\ell)| = |\langle A - \hat{A}, \nabla w_\ell \cdot \nabla v_\ell \rangle_H|. \tag{24}$$

Hence, for a fixed discretization level ℓ, we have $\nabla w_\ell \cdot \nabla v_\ell \in H$ and as a consequence it is sufficient to have that $\hat{A}$ converges weakly to A in the H topology to control the error in (24)*. In particular, it suffices that $\hat{A} \to A$ strongly in H instead of stronger convergence in $L^2(\Omega; L^\infty(D))$ or $L^Q(\Omega; L^q(D))$, when starting from the discrete setting at the cost of an unknown convergence rate.*

3. SURROGATE RESPONSE

The construction of surrogate models for problems with high-dimensional input (parameters) becomes essential when extensive sampling is computationally expensive in comparison to the construction of adequate functional approximations. These may even be viable for non-smooth data since it can still be possible to exploit local smoothness, which then results in sufficiently accurate surrogates (in certain parameter subdomains).

In the literature there is a vast amount of surrogate types, including generalized polynomial chaos expansions (gPCE), *e.g.* [49, 19], its multi-element extension, *e.g.* [48], low-rank [26, 22] and sparse grid techniques, *e.g.* [38, 23] or neural networks.

A central motivation for the proposed approach is the treatment of parametric composite materials. With this in mind, our aim is to build (local) surrogates for (local) maps within a domain decomposition framework presented in Section 4. For this, we focus on two surrogate types based on a parameter space decompostion, namely the *multi-element generalized polynomial chaos* expansion and a *partition of unity interpolation*. The advantages of these approaches is the ability to explore areas in the parameter domain in which the underlying maps are more regular. In the case of low-rank structures, also hierarchical tensor representations might become useful, which we defer to future research.

3.1. **Surrogates for matrix valued functions.**

In preparation of the framework of localized descriptions of randomness in a domain decomposition setup, we discuss different surrogate models for random matrices of the form

$$\boldsymbol{\xi}^r(\omega) \mapsto M^s(\boldsymbol{\xi}^r(\omega)) \in \mathbb{R}^{n,m}, \tag{25}$$

for some indices $r, s \in \mathbb{N}$. In our application, n and m depend on the number of interface degrees of freedom or subsets of these. The choice of surrogate for the map (25) should be made dependent on the regularity of the involved map. In particular, we have the following surrogates in mind that are based on (quasi-) best approximations or interpolations:

1 *hPCE surrogates*: A set of piecewise orthonormal polynomials w.r.t. an underlying measure is constructed, see section 3.2. The coefficients in the hPCE series are computed via projection, or (sparse) quadrature schemes.
2 *Hierarchical tensor surrogates*: A number of samples of M^s and a given underlying discrete tensor basis is provided. Then, a tensor reconstruction as in the (non-intrusive) *Variational Monte Carlo method* [18] yields a L^2-compressed low-rank representation.
3 *PoU interpolation surrogates*: Based on an adaptive mesh of Γ_k, a discrete partition of unity basis with respect to the mesh is used. This can e.g. be obtained by a LAGRANGE basis with respect to mesh nodes. Each basis coefficient is computed by a single sample. More details are provided in Section 3.3.
4 *Sparse grid interpolation surrogates* are build by evaluating a realization of M^s on each sparse grid point.

Remark 3.1. *In the case of low regularity of the map* (25) *and no knowledge of a basis for an approximation scheme with (quasi)-optimal convergence in the sense of ℓ^p-summability of coefficients for some $p \geq 1$* [4]*, one may be restricted to lower local parametric dimensions to obtain an affordable and accurate surrogate.*

While out of the scope of this paper, a progressive learning of an approximate basis as *e.g.* via a *Neural Network regression* might be useful, given its training only involves a manageable number of samples.

3.2. **Generalized Multi-Element Polynomial Chaos Expansion.** The following presentation is motivation by the approximation of non-smooth functions, where standard functional approaches may lack efficiency due to the GIBBS phenomenon.

We consider a probability measure μ on $\Xi \subset \mathbb{R}^{M'}$ and the space $L^2(\Xi, \mathcal{B}(\Xi), \mu)$. For the envisaged application, Ξ (or Ξ^r) is the image and μ will be the push-forward of $\mathbb{P}$ of an underlying parameter random vector. Let $\mathcal{I} = \mathbb{N}$ and assume that there exists a family of orthonormal polynomials $\Psi := \{\psi_\alpha\}_{\alpha \in \mathcal{I}}$, s.t. $\operatorname{span} \Psi$ is dense in $L^2(\Xi, \mathcal{B}(\Xi), \mu)$. Note that if there exists $c > 0$ and a norm $\|\cdot\|$ on $\mathbb{R}^{M'}$ such that

$$\int_\Xi e^{c\|\mathbf{y}\|} \mathrm{d}\mu(\mathbf{y}) < \infty, \tag{26}$$

then such a family does indeed exist [12].

Example 3.2. *The condition* (26) *holds for any bounded domain Ξ or for $\Xi = \mathbb{R}^{M'}$ and any* GAUSSIAN *measure μ including the non-independent case* [39].

In case that μ exhibits a product structure, *i.e.* the *independent case*, the index set $\mathcal{I}$ can be reshaped into a multi-index tensor structure. The existence of a complete orthornormal polynomial basis then may be answered via the HAMBURGER moment problem [12].

Remark 3.3. *There exist probability measures such that no dense polynomial subset exists. A classical example is the log-normal case. For $M' > 1$ and a non-separable probability measure μ or a non-tensorized domain Ξ, such a family of polynomials may exist but is not necessarily unique* [12].

We now consider a finite non-overlapping partition of $\Xi = \bigcup_{k\in\mathcal{J}} \Xi_k$ with $|\mathcal{J}| < \infty$, $\Xi_k \in \mathcal{B}(\Xi)$ and $0 < \mu(\Xi_k) \leq 1$. This gives rise to the decomposition

$$Y := L^2(\Xi, \mathcal{B}(\Xi), \mu) = \bigoplus_{k\in\mathcal{J}} Y_k, \quad Y_k := \{v \in L^2(\Xi, \mathcal{B}(\Xi), \mu) : \operatorname{supp}(v) \subset \Xi_k\}.$$

Lemma 3.4. *There is a family of orthonormal polynomials that spans a dense subset in Y_k.*

Proof. Fix $v \in Y_k$ and $\epsilon > 0$. Let χ_k denote the indicator function with respect to Ξ_k, then $\varphi_{\alpha,k} := \chi_k\psi_\alpha$ for $\alpha \in \mathcal{I}$ is a polynomial in Y_k. Let Ψ_k be an orthonormalized version of $\Pi_k := \{\varphi_{\alpha,k}, \alpha \in \mathcal{I}\}$ with respect to the inner product in Y_k. Since Ψ is dense in Y, there exists $\mathcal{I}_\epsilon \subset \mathcal{I}$, $|\mathcal{I}_\epsilon| < \infty$ and a polynomial $\psi_\epsilon \in \operatorname{span}\Psi$ with $\|E_0^k v - \psi_\epsilon\|_{L^2(\Xi,\mathcal{B}(\Xi),\mu)} < \epsilon$. Here, $E_0^k \colon L^2(\Xi_k) \to L^2(\Xi)$ denotes the zero extension operator. Consequently $\|v - \chi_k\psi_\epsilon\|_{Y_k} < \epsilon$, where $\chi_k\psi_\epsilon \in \operatorname{span}\Psi_k$. □

Motivated by Lemma 3.4, we define an (weak) orthonormal polynomial set

$$\Psi_k := \{\psi_{\alpha,k}, \alpha \in \mathcal{I}, \psi_{\alpha,k} \text{ is polynomial}\}, \quad (\psi_{\alpha,k}, \psi_{\alpha',k})_{Y_k} = \delta_{\alpha,\alpha'}, \tag{27}$$

which spans a dense subset in Y_k. We note that in the independend case the decomposition of Ξ has to respect the tensor structure to obtain a product structure of the polynomial chaos.

Lemma 3.5. *$\bigoplus_{k\in\mathcal{J}} \Psi_k$ spans a dense subset in Y with Ψ_k.*

As the partition of Ξ can be interpreted as a possibly non-regular meshing, we abbreviate the construction of polynomial chaos on several elements as *gHPCE*, motivated by hp-FEM in the standard LEBESGUE spaces $L^2(D, \mathrm{d}\lambda)$. For more details on the existence of dense generalized polynomial chaos we refer to [49, 19, 12].

We end this subsection with an instructive example.

Example 3.6. *(Construction of gHPCE) Consider the special case of $\Xi \subset \mathbb{R}$ and denote by $\frac{\mathrm{d}\mu}{\mathrm{d}y} = \varrho$ the* RADON-NIKODÝM *derivative of μ with respect to the* LEBESGUE *measure. Let $a_0 = \inf \Xi < a_1 < \ldots < a_{|\mathcal{J}|} := \sup \Xi$. Then, orthornormal polynomial families in $L^2([a_k, a_{k+1}], \varrho)$ can be obtained by a* GRAM-SCHMIDT *procedure . In the case of a uniform distribution, the multi-element* LEGENDRE *chaos can be obtained by simple rescaling and translation of standard Legendre chaos.*

3.3. **Surrogates based on PoU-Interpolation.** Let $\Xi^r := \operatorname{img}\boldsymbol{\xi}^r$ and assume a nested set of discrete function spaces

$$U_{s,0}^r \subset U_{s,\ell}^r \subset \ldots \subset U_{s,L}^r \tag{28}$$

of level $\ell = 0, 1, \ldots, L$, defined by

$$U_{s,\ell}^r := \{\varphi_k^{s,\ell} \colon \Xi^r \to \mathbb{R}, k = 1, \ldots, N_\ell^i < \infty\}, \tag{29}$$

such that its elements form a *partition of unity* (PoU) on Ξ^r, *i.e.* $\sum_{k=1}^{N_\ell^i} \varphi_k^{s,\ell} \equiv 1$. To describe an important class of this spaces, we consider a family of cell partitions $\mathcal{M}_\ell^r$ of level $\ell = 1, \ldots, L$ of Ξ^r with tree structure: for each cell in $\mathcal{M}_{\ell+1}^r$ there is a unique father cell in $\mathcal{M}_\ell^r$. Furthermore, assume that for each $k = 1, \ldots, N_\ell$ the function $\varphi_k^{s,\ell}$ has support in one cell in $\mathcal{M}_{\ell+1}^r$ only, i.e.

$$\forall k = 1, \ldots, N_\ell, \exists! \, T \in \mathcal{M}_\ell^r : \operatorname{supp}\varphi_k^{s,\ell} \subset T. \tag{30}$$

We associate with each such function in $U_{s,\ell}^r$ a *global degree of freedom* and a unique associated element in Ξ^r denoted by *global coordinate degree of freedom*.

With these constructions we formulate an adaptive scheme to build up surrogates for the parametric matrix ensemble in Algorithm 1, used in our numerical experiments. The aim of the proposed algorithm is to balance the maximization the trust region while keeping the creation process as cheap as possible.

Algorithm 1 Hybrid surrogate based on Partition of Unity

Input: ∘ sampler $\mathcal{S}$ for parametric matrix $M^s(\boldsymbol{\xi}^r(\omega))$
∘ surrogate quality parameter $tol > 0$
∘ maximal level of refinement L
Output: hybrid surrogate for $\boldsymbol{\xi}^r(\omega) \mapsto M^s(\boldsymbol{\xi}^r(\omega))$.

```
init M_0^r, U_{s,0}^r
for all ℓ = 0, ..., L do
    init markings/ trust region / non trust region as ∅
    for all global (coordinate) d.o.fs of U_{s,ℓ}^r do
        evaluate S and assign it to the corresponding global d.o.f.
    end for
    for all T ∈ M_ℓ^r do
        judge quality of current surrogate on T w.r.t tol and set T to be trusted / not trusted
        update trust region / non trust region with T
        if T is not trusted then
            mark T in (M_ℓ^r, U_{s,ℓ}^r) for refinement, i.e. add to markings
        end if
    end for
    if markings = ∅ then break
    else M_{ℓ+1}^r, U_{s,ℓ+1}^r := refine( M_ℓ^r, U_{s,ℓ}^r, markings)
end for
return hybrid surrogate: defined in U_ℓ^r for input within trust region and else coincides with S.
```

Remark 3.7. *The hybrid structure, namely letting the surrogate coincide with a sample on the non trust region, allows to control the cost of creating the surrogate in L iterations. For large L, this leads to overrefinement and thus too many sampler calls.*

Remark 3.8. *Although the above representation is presented for matrices, the technique also extends to matrices given only implicitly: If we are interested in building a surrogate for $\boldsymbol{\xi}(\omega) \mapsto A(\boldsymbol{\xi}(\omega))^{-1}$, due to the partition of unity approach, for each global coordinate degree of freedom we store a LU factorization only. Then, the evaluation of the surrogate at a point p requires several forward-backward substitutions associated to all basis functions evaluating to non-zero at p. Note that here each LU decomposition may have its own sparsity pattern determined by its pivotization and scaling.*

4. Parametric Domain decomposition

Based on an abstract mode given in terms of a partial differential equation with possible high-dimensional random input decomposed with respect to a physical partition, we present a domain decomposition framework that leads to local problems with lower parametric dimensions. Based on a semi-discretization, we introduce an accelerated sampling scheme in the spirit of [11], which employs an adaptive construction of surrogates of local parameteric interface operators.

4.1. Abstract random domain decomposed model.

Consider a partition of D into mutual disjoint, non-empty connected Lipschitz subdomains $D_s \subset D$, $s = 1, \dots, N_{\mathrm{SD}} < \infty$. We are interested in random fields given in parameterized form and possibly localized with respect to $(D_s)_s$. Such local respresentations of random fields may for instance occur in the following scenarios

- Localization to D_s via Karhunen-Loève expansion (KLE), *e.g.* [10, 5], in case of underlying Gaussian random fields, see Example 4.2.
- Local uncertainties, *e.g.* the random composite material model from Example 2.9.

Instead of an abstract random field $A(x, \omega)$, we consider a parametrization by a given stochastic coordinate system represented by some $\boldsymbol{\xi} \colon \Omega \to \mathbb{R}^{M'}$, $M' \in \mathbb{N} \cup \{\infty\}$. Let $\sigma(\boldsymbol{\xi}) \subset \mathcal{U}$ be the sigma algebra generated by $\boldsymbol{\xi}$ and $(\Omega, \sigma(\boldsymbol{\xi}), \mathbb{P})$ the considered probability space. Furthermore, assume a sub-enumeration of the M'-dimensional random vector $\boldsymbol{\xi}$ into $M \leq N_{\mathrm{SD}}$ blocks of m_r-dimensional

(sub) random vectors $\boldsymbol{\xi}^r : \Omega \to \mathbb{R}^{m_r}$ with $1 \leq m_r \leq M'$ and components $\xi_i^r := (\boldsymbol{\xi}^r)_i, i = 1, \dots, m_r, r = 1, \dots, M$. We are then interested in a physical model described by a linear PDE with randomness modelled by $\boldsymbol{\xi}$ where at most one input random sub-vector $\boldsymbol{\xi}^r$ acts on a subdomain D_s as illustrated in Figure 2. If the latter is the case, we call the tuple (r, s) an *active index*, which we collect in

$$\mathcal{I}_{\text{active}} := \{(r,s) \in \{1,\dots,M\} \times \{1,\dots N_{\text{SD}}\} : (r,s) \text{ is active index}\}. \tag{31}$$

The abstract equations reads for a.a. $\omega \in \Omega$

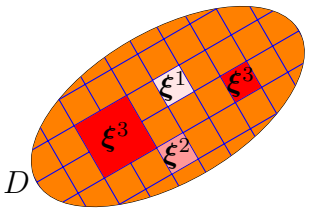

FIGURE 2. Parametric random input given by $M = 4$ sub random vectors $\boldsymbol{\xi}^r, r = 1, \dots, 4$ distributed over different sub-structures.

$$\mathcal{L}(\boldsymbol{\xi}(\omega), x)u(\boldsymbol{\xi}(\omega), x) = f(x), \qquad \text{in } D, \tag{32}$$

$$\mathcal{B}(\boldsymbol{\xi}(\omega), x)u(\boldsymbol{\xi}(\omega), x) = g(x), \qquad \text{on } \Gamma, \tag{33}$$

with $\mathcal{L}(\boldsymbol{\xi}(\omega), x) = \mathcal{L}(\boldsymbol{\xi}^r(\omega), x)$ for $x \in D_s$ for each $(r, s) \in \mathcal{I}_{\text{active}}$ from (31) and $\mathcal{L}(\boldsymbol{\xi}(\omega), x) = \mathcal{L}(x)$ else. An analog structure holds for the boundary operator $\mathcal{B}$. Here, we assume existence and uniqueness of a solution $u \in L^2(\Omega, \sigma(\boldsymbol{\xi}), \mathbb{P}) \otimes \mathcal{V}$ for some separable Hilbert space $\mathcal{V}$, *e.g.* $\mathcal{V} = H^1_{\Gamma_{\text{D}}}(D)$ in the case of (1). Note that the abstract model includes several important cases of random modeling:

- Direct modeling with independent random components, *i.e.* $(\boldsymbol{\xi}^s)_s$ are mutually independend random vectors and $\mathcal{L}$ is defined by material parameters that depend locally on $\boldsymbol{\xi}^r$ in a possibly non-linear manner.
- The setting $\boldsymbol{\xi}^r \equiv \boldsymbol{\xi}$ corresponds to global random contributions, which includes the non-localized (standard) KLE case.
- The local coordinates $\boldsymbol{\xi}^r$ are obtained by a localized KLE. In the case that the underlying random field is GAUSSian, $\boldsymbol{\xi}$ and $\boldsymbol{\xi}^r$ consist of mutually independend GAUSSian random variable components, although now $(\boldsymbol{\xi}^r)_r$ is not independent in general.
- The case of one localized uncertainty input $M = 1$ as in [8].

Remark 4.1. *In order to balance the workload for parallel computations in the domain decomposition schemes introduced by varying sizes of subdomains described below, one might decompose a large subdomain, e.g. D_s, with operator dependence only on $\boldsymbol{\xi}^r$, $(r, s) \in \mathcal{I}_{\text{active}}$ into $D_s = D_{s'} \cup D_{s''}$, thus updating $\mathcal{I}_{\text{active}}$ with $(r, s'), (r, s'')$ instead of (r, s). This may require more involved system preconditioners since the material coefficient on the interface $D_{s'} \cap D_{s''}$ might behave non-trivially.*

Example 4.2. *(**localized Karhunen-Loève expansion**,* [10]*)*
Given the mean and covariance kernel, a random field $A = aI$ may be written via KLE as

$$a(x, \omega) = a(x, \boldsymbol{\eta}(\omega)) = a_0(x) + \sum_{i=1}^{\infty} \sqrt{\lambda_i} a_i(x) \eta_i(\omega), \quad x \in D,$$

with centered, uncorrelated random variables η_i and eigenpairs (λ_i, a_i) of the underlying covariance operator with respect to the full domain D. When considering the eigenvalue problem on subdomains

D_s only, we obtain local representations in a new (larger) coordinate system $\boldsymbol{\xi} = (\boldsymbol{\xi}^s)_{s=1}^{N_{SD}}$ with sub-coordinates $\boldsymbol{\xi}^s = (\xi_i^s)_{i\in\mathbb{N}}$, i.e. $\mathcal{I}_{active} = \{(s,s) : s = 1,\dots N_{SD}\}$ and

$$a(x,\omega) = a(x,\boldsymbol{\xi}^s(\omega)) = a_0(x) + \sum_{j=1}^{\infty} \sqrt{\lambda_j^s} a_j^s \xi_j^s(\omega), \quad x \in D_s.$$

Assume that the global KLE truncated after M terms yields the desired accuracy. In the case that the local eigenvalues $(\lambda_j^s)_j$ have a (much) lower magnitude, the local KLE can be truncated after $m_s \ll M$ terms, i.e. a low dimensional local representation of the random field. Furthermore, there exists a matrix $A^s \in \mathbb{R}^{m_s,M}$ such that $(\eta_j^s)_{j=1}^{m_s} = A^s(\xi_i)_{i=1}^M$. In the case of GAUSS*ian random fields, one gets the favourable property that (η_j^s) are independent* GAUSS*ian random variables as well, enabling local dense polynomial chaos approximations. Note however that $(\boldsymbol{\xi}^s)_s$ is not independent in general.*

Remark 4.3. *Contrary to example 4.2, in the case that $(\eta_i)_{i=1}^M$ are independent non-*GAUSS*ian random variables, the distribution of $(\xi_j^s)_{j=1}^{m_s}$ can be arbitrarily complex since the involved linear map A^s introduces a non-linear mapping of distributions due to $m_s < M$. Hence, one cannot expect $(\xi_j^s)_{j=1}^{m_s}$ to be independent and the existence of a dense polyomial chaos in $L^Q(\Omega, \sigma(\boldsymbol{\xi}^s), \mathbb{P})$ is not ensured in general, e.g. if $\operatorname{img} \boldsymbol{\xi}^s \subset \mathbb{R}^{m_s}$ is unbounded. Note that the image might be of lower topological dimension, e.g. a submanifold only.*

4.2. **Parametric hybrid domain decomposition based on semi-discretization.** Domain decomposition generally refers to the splitting of a PDE or an approximation thereof into coupled problems on smaller subdomains, forming a partition of the original domain, see [46]. We present the framework on a semi-discrete formulation with regard to some suitable discrete subspace of $\mathcal{V}$. Then, the structure of the decomposed random model (32)-(33) results in a random system of equations

$$\mathcal{A}(\boldsymbol{\xi}(\omega))u(\boldsymbol{\xi}(\omega)) = F(\boldsymbol{\xi}(\omega)). \tag{34}$$

The domain decomposition approach for random PDEs is applied in the context of global and local Karhunen-Loève expansions in [43] and [11] with a combination of model reduction techniques [37] for the SCHUR complement or the FETI-DP method. We note that the technique based on global random coordinates as in [43] is based on a stochastic FE formulation without a sampling stage, which limits it to a moderate number of random coordinates due to the curse of dimensionality. The analysis and application of hierachical tensor formats in this context is defered to future research. To alleviate the issue of moderate dimensions, our aim is to rely on local random coordinates only, *e.g.* based on canonical tensor representations as in [27]. In what follows, we present both techniques, the SCHUR complement and the FETI-DP method based on adaptively constructed local surrogates that enable accelerated sampling. The devised general hybrid approach is summarized in Algorithm 2.

Remark 4.4. *If the local representation of $\mathcal{L}(\boldsymbol{\xi}^r(\omega), x)$ is given by means of a gPCE with independent (ξ_k^r) then the involved local random operators may be represented in low-rank formats as in* [15]*, allowing for higher dimensional local input. This approach transfers to compressed structures of all involved parametric suboperators.*

4.2.1. *Parametric Schur complement method.* As a first approach to non-overlapping domain decomposition methods, we consider the SCHUR complement method, see *e.g.* [46, Ch. 4-5] for details. For simplicity, the presentation is based on the elliptic linear equation (1) with the random dependence setting introduced in the beginning of this section. Given a physical discretization space $V_h \subset \mathcal{V} := H^1_{\Gamma_0}(D)$ spanned by a nodal LAGRANGE basis on a matching triangle (tetrahedral for $d = 3$) mesh of D, we consider a semi-discretization with respect to the physical coordinate $x \in D$.

Algorithm 2 Abstract hybrid domain decomposition

Input: ○ number of total samples N
○ local discrete physical spaces $V_{h,s}$
○ surrogate cost bound $C_\$$ and desired accuracy tol
Output: Sample based approximation of some Q.o.I.(u).
for all active pair (r,s) subdomain D_s in parallel **do**
  if surrogate creation cost $< C_\$$ **then**
    createLocalSurrogates($V_{h,s}$, semi-discrete PDE, tol)
  else
    createLocalSampler($V_{h,s}$, semi-discrete PDE, matrix free=true)
  end if
end for
for all sample $\boldsymbol{\xi}_k$, $k=1,\dots,\mathrm{N}$ in parallel **do**
  obtain local samples $(\boldsymbol{\xi}_k^r)_{r=1}^M$ from $\boldsymbol{\xi}_k$
  solve global interface problem(s) via parallel application of $\mathcal{S}^s(\boldsymbol{\xi}_k^r)$ for $s=1,\dots,N_{\mathsf{SD}}$
  solve full decoupled local problems in parallel for $s=1,\dots,N_{\mathsf{SD}}$
  add solution sample contribution to approximate $Q.o.I.(u)$
end for

Let us denote by Π the (primal) *interface*

$$\Pi = \cup_{s\neq s'} \partial D_s \cap \partial D_{s'},$$

consisting of faces ($d=3$), edges and vertices with respect to the underlying mesh. Identifying the degrees of freedoms in V_h with topological entities, these can be reordered with regard to *local* contributions indexed by the letter L, corresponding to topological entities in the inner of D_s and on Neumann parts $\partial D_s \cap \Gamma_1$ and to interacting primal interface contributions indexed by the letter Π, for convenience. This semi-discretization of (1) leads to the structure (34) with

$$\mathcal{A}(\boldsymbol{\xi}(\omega)) := \begin{pmatrix} A_{LL} & A_{L\Pi} \\ A_{\Pi L} & A_{\Pi\Pi} \end{pmatrix}(\boldsymbol{\xi}(\omega)), \quad u(\boldsymbol{\xi}(\omega)) := \begin{pmatrix} u_L \\ u_\Pi \end{pmatrix}(\boldsymbol{\xi}(\omega)), \quad F := \begin{pmatrix} f_L \\ f_\Pi \end{pmatrix}.$$

Block GAUSSian elimination leads to an equivalent system to (34) given by

$$\tilde{\mathcal{A}}(\boldsymbol{\xi}(\omega))u(\boldsymbol{\xi}(\omega)) = \tilde{F}(\boldsymbol{\xi}(\omega)), \tag{35}$$

where

$$\tilde{\mathcal{A}}(\boldsymbol{\xi}(\omega)) := \begin{pmatrix} A_{LL} & A_{L\Pi} \\ 0 & S_{\Pi\Pi} \end{pmatrix}(\boldsymbol{\xi}(\omega)), \quad \tilde{F}(\boldsymbol{\xi}(\omega)) := \begin{pmatrix} f_L \\ \tilde{f}_\Pi(\boldsymbol{\xi}(\omega)) \end{pmatrix},$$

with $\tilde{f}_\Pi(\boldsymbol{\xi}(\omega)) := f_\Pi - A_{\Pi L}(\boldsymbol{\xi}(\omega))A_{LL}(\boldsymbol{\xi}(\omega))^{-1}f_L$. Let R_s be the rectangular restriction matrix which restricts the global degrees of freedom vector associated to Π to local degrees of freedom vectors associated to local interface entities on the mesh on D_s only. Since the mesh has no hanging nodes, the entries of each R_s are in $\{0,1\}$. For each $s=1,\dots,N_{\mathsf{SD}}$, consider local assembled matrices $A_{LL}^s, A_{L\Pi}^s, A_{\Pi,L}^s, A_{\Pi\Pi}^s$, associated to local physical discretization spaces on D_s. Note that for each active index (r,s) these matrices have a parametric dependence on $\boldsymbol{\xi}^r$. With the given ordering in (31), it follows that these matrices are given by

$$\begin{aligned} A_{LL}(\boldsymbol{\xi}(\omega)) &= \mathrm{blockdiag}(A_{LL}^1,\dots,A_{LL}^s,\dots,A_{LL}^{N_{\mathsf{SD}}}), \\ A_{\Pi L}(\boldsymbol{\xi}(\omega)) &= \mathrm{blockdiag}(R_1,\dots,R_{N_{\mathsf{SD}}})\left[A_{\Pi L}^1,\dots A_{\Pi L}^s,\dots,A_{\Pi L}^{N_{\mathsf{SD}}}\right], \\ S_{\Pi\Pi}(\boldsymbol{\xi}(\omega)) &= \sum_{s=1}^{N_{\mathsf{SD}}} R_s S_{\Pi\Pi}^s R_s^T, \quad S_{\Pi\Pi}^s = A_{\Pi\Pi}^s - A_{\Pi L}^s A_{LL}^{s^{-1}} A_{L\Pi}^s, \end{aligned}$$

where each matrix with index s only depends on $\boldsymbol{\xi}^r(\omega)$ if $(r,s) \in \mathcal{I}_{\text{active}}$ and $A_{\Pi L} = A_{L\Pi}$ almost everywhere in Ω. In particular, for each active index (r,s), we have

$$S_{\Pi\Pi}^s(\boldsymbol{\xi}^r(\omega)) = A_{\Pi\Pi}^s(\boldsymbol{\xi}^r(\omega)) - A_{\Pi L}^s(\boldsymbol{\xi}^r(\omega))A_{LL}^s(\boldsymbol{\xi}^r(\omega))^{-1}A_{L\Pi}^s(\boldsymbol{\xi}^r(\omega)). \tag{36}$$

In the deterministic setting, (35) is solved by first iteratively solving for u_Π and second solving (in parallel) for interior contributions u_L^s with $u_L = [u_L^1, \dots, u_L^{N_{\text{SD}}}]$. The full matrix $S_{\Pi\Pi}$ is never formed explictly. Its action on a vector involves the application of the smaller matrices $S_{\Pi\Pi}^s$. In the determinstic case, the latter might be realized by a LU decomposition of A_{LL}^s and we build local surrogate models $\hat{S}_{\Pi\Pi}^s \approx S_{\Pi\Pi}^s$. Depending on the regularity of the maps

$$\boldsymbol{\xi}^r(\omega) \mapsto S_{\Pi\Pi}^s(\boldsymbol{\xi}^r(\omega)) \tag{37}$$

and the input dimension of $\boldsymbol{\xi}^r$, this might be realized by interpolation (e.g. sparse grid, LAGRANGE interpolation) or (quasi-)best approximation techniques (tensor reconstruction, hPCE). We note that the construction of the surrogate models may be expensive if the number of local degrees of freedom associated with Π or the random dimension of $\boldsymbol{\xi}^r$ grows or if there is a lack of regularity. In a practical implementation, this cost factor has to be compared to the cost of a full sampling approach with several backward and forward solves of the involed LU decompositions in the iterative process of the application of the SCHUR complement matrix. It is known that the condition number of a deterministic SCHUR complement matrix grows like $\mathcal{O}(1/Hh)$, where H is the diameter of the subdomains and h the maximal element size in the subdomains [46].

The proposed method is summarized in Algorithm 3.

Algorithm 3 Realization as parametric SCHUR complement method

Input: ○ sample $\mathbf{y}_k := \boldsymbol{\xi}_k(\omega) = [\boldsymbol{\xi}_k^1, \dots, \boldsymbol{\xi}_k^M](\omega)$,
○ local system surrogates for $\boldsymbol{\xi}(\omega) \mapsto S_{\Pi\Pi}(\boldsymbol{\xi}(\omega))$
○ local surrogates for preconditioner of (parametric) $S_{\Pi\Pi}$.

Output: approximated realization of $u_k = u(\boldsymbol{\xi}_k(\omega))$ or of subdomain parts $u_k^s = u_{k|D_s}$.

1: Compute right-hand side realization $\tilde{F}_k = [f_L, \tilde{f}_{\Pi,k}] = \tilde{F}(\boldsymbol{\xi}_k(\omega))$ of (35) via system surrogates.
2: Iterativly solve $S_{\Pi\Pi,k} u_{\Pi,k} = \tilde{f}_{\Pi,k}$ via PCG. The application of operator $S_{\Pi\Pi,k}$ and its preconditioner are based on evaluation of local surrogates.
3: Solve block diagonal system $A_{LL,k} u_{L,k} = f_L - A_{L\Pi,k} u_{\Pi,k}$ in parallel.

4.2.2. *Parametric FETI-DP.* The *Finite Element Tearing* and *Interconnecting Dual-Primal* (FETI-DP) method is known to successfuly balance the requirement of a minimal communication by a coarse space by keeping good convergence rates within the preconditioned conjugate gradient solution scheme. It was introduced in [20] and further developed in [46, 41, 40, 32, 31], see also the references therein for the purely deterministic case. The main idea is to translate the original problem into a dual problem in which the local iterates are not conforming (*e.g.* discontinous in the H^1 framework), represented by most degrees of freedom (d.o.f.s) associated with the domain interfaces. Only a small number is strongly enforced to be conforming (*e.g.* continuous) opposite to the SCHUR complement method, where all (primal) d.o.f.s associated with the interface are globally constrained. This small number of constraints is associated with *primal* d.o.f.s for building the (global) coarse communication space. To enforce conformity of the method, the iteration solves for *Lagrange* multipliers λ , which construct the *dual variables*. In the case of convergence, this enforces conformity of the non-primal interface degrees of freedom. For further extensions of the coarse space design, *e.g.* including adaptivity, we refer to [30, 33].

For the sake of simplicity, we stay on the algebraic matrix level subject to the discretization of the symmetric model problem (1). For interpretation in a HILBERTian framework, we refer to [35] and for a formulation in intermediate approximation FE spaces to [46].

After choosing the interior, dual and primal degrees of freedom indexed by the subindices I, Δ and Π for a given physical discretization based on meshes on D_s that are aligned with each other on the

subdomain interfaces, the structure of the system (34) is given by

$$\mathcal{A}(\boldsymbol{\xi}(\omega)) := \begin{pmatrix} A_{LL} & A_{L\Pi} & \mathcal{J}_L^T \\ A_{\Pi L} & A_{\Pi\Pi} & \mathcal{J}_\Pi^T \\ \mathcal{J}_L & \mathcal{J}_\Pi & 0 \end{pmatrix}(\boldsymbol{\xi}(\omega)), \quad u(\boldsymbol{\xi}(\omega)) := \begin{pmatrix} u_L \\ u_\Pi \\ \lambda \end{pmatrix}, \quad b = \begin{pmatrix} f_L \\ f_\Pi \\ 0 \end{pmatrix}.$$

Here, the subindex $L = [I, \Delta]$ merges the subindices I and Δ to *local* contributions. The jump operators $\mathcal{J}_L = [\mathcal{J}_L^1, \dots, \mathcal{J}_L^{N_{\mathsf{SD}}}]$ with $\mathcal{J}_L^s = [0, J_\Delta^s]$ and $\mathcal{J}_\Pi$ consisting of values in $\{-1, 0, 1\}$ are build such that the solution vector $[u_L, u_\Pi]$ yields a conforming approximation if $[\mathcal{J}_L, \mathcal{J}_\Pi][u_L, u_\Pi]^T = 0$. Introducing restriction operators R_Π^s similar to the SCHUR complement method, mapping local primal degrees of freedom to global d.o.f.s associated with index Π, sub-assembling with respect to the primal variables (thus eliminating the need of $\mathcal{J}_\Pi$) and application of GAUSSian block elimation leads to an equivalent formulation that reads

$$\tilde{\mathcal{A}}(\boldsymbol{\xi}(\omega))\tilde{u}(\boldsymbol{\xi}(\omega)) = \tilde{b}(\boldsymbol{\xi}(\omega)), \tag{38}$$

where

(39)
$$\tilde{\mathcal{A}}(\boldsymbol{\xi}(\omega)) := \begin{pmatrix} A_{LL} & \tilde{A}_{L\Pi} & \mathcal{J}_L^T \\ 0 & \tilde{S}_{\Pi\Pi} & -\tilde{S}_{\Pi\lambda} \\ 0 & 0 & F \end{pmatrix}(\boldsymbol{\xi}(\omega)), \quad \tilde{u}(\boldsymbol{\xi}(\omega)) := \begin{pmatrix} u_L \\ \tilde{u}_\Pi \\ \lambda \end{pmatrix}, \quad \tilde{b}(\boldsymbol{\xi}(\omega)) := \begin{pmatrix} f_L \\ \tilde{b}_\Pi(\boldsymbol{\xi}(\omega)) \\ \tilde{b}_\lambda(\boldsymbol{\xi}(\omega)) \end{pmatrix}.$$

Here, it holds that $\tilde{u}_\Pi = \sum_{s=1}^{N_{\mathsf{SD}}} R_\Pi^s u_\Pi^s$, with $u_\Pi = [u_\Pi^1, \dots, u_\Pi^{N_{\mathsf{SD}}}]$, stemming from a rearrangement of global degrees of freedom. For $s = 1, \dots, N_{\mathsf{SD}}$, similar to the SCHUR complement method, we introduce the locally assembled semi-discrete matrices $A_{LL}^s, A_{L\Pi}^s, A_{\Pi,L}^s, A_{\Pi\Pi}^s$ with dependence only on $\boldsymbol{\xi}^r(\omega)$ if $(r, s) \in \mathcal{I}_{\text{active}}$. We then have the relation

$$\tilde{S}_{\Pi\Pi}(\boldsymbol{\xi}(\omega)) := \tilde{A}_{\Pi\Pi} - \tilde{A}_{\Pi L} A_{LL}^{-1} \tilde{A}_{L\Pi} = \sum_{s=1}^{N_{\mathsf{SD}}} R_\Pi^s \left(A_{\Pi\Pi}^s - A_{\Pi L}^s A_{LL}^{s^{-1}} A_{L\Pi}^s \right) {R_\Pi^s}^T,$$

$$\tilde{S}_{\Pi\lambda}(\boldsymbol{\xi}(\omega)) := \tilde{A}_{\Pi L} A_{LL}^{-1} \mathcal{J}_L^T = \sum_{s=1}^{N_{\mathsf{SD}}} R_\Pi^s A_{\Pi L}^s A_{LL}^{s^{-1}} \mathcal{J}_L^{sT},$$

with the random FETI-DP dual matrix F and right-hand side contributions such that

$$F(\boldsymbol{\xi}(\omega)) := \mathcal{J}_L A_{LL}^{-1} \mathcal{J}_L^T + \tilde{S}_{\Pi\lambda}^T \tilde{S}_{\Pi\Pi}^{-1} \tilde{S}_{\Pi\lambda},$$

$$\tilde{b}_\Pi(\boldsymbol{\xi}(\omega)) := \sum_{s=1}^{N_{\mathsf{SD}}} R_\Pi^s (f_\Pi^s - A_{\Pi L}^s A_{LL}^{s^{-1}} f_L^s),$$

$$\tilde{b}_\lambda(\boldsymbol{\xi}(\omega)) := \mathcal{J}_L A_{LL}^{-1} f_L - \tilde{S}_{\Pi\lambda}^T \tilde{S}_{\Pi\Pi}^{-1} \tilde{b}_\Pi.$$

Note that for better readability we omit the parametric dependence of matrices on the right-hand sides of the above equations. Examining the occurring matrices, their dimensions and their random dependence on local random vectors $\boldsymbol{\xi}^s(\omega)$, we now discuss the construction of surrogate models. In order to avoid multiple LU forward and backward substitutions in the iteration of the system $F\lambda = \tilde{b}_\lambda$, we aim for a lower total cost of computing and storing the surrogates for a given total number of samples. The parametric matrix F contains three contributions, which are discussed separately:

- With the random dependence $A_{LL}^s = A_{LL}^s(\boldsymbol{\xi}^r(\omega)), (r, s) \in \mathcal{I}_{\text{active}}$, recall that

$$\mathcal{J}_L A_{LL}^{-1} J_L^T = \sum_{s=1}^{N_{\mathsf{SD}}} \mathcal{J}_L^s A_{LL}^{s^{-1}} \mathcal{J}_L^{sT}, \quad \mathcal{J}_L^s = [0, \mathcal{J}_\Delta^s].$$

The inverse of A_{LL}^s can be seen as a 2×2 block matrix

$$A_{LL}^{s^{-1}} = \begin{pmatrix} B_{II}^s & B_{I\Delta}^s \\ B_{\Delta I}^s & B_{\Delta\Delta}^s \end{pmatrix}. \tag{40}$$

Due to the design of $\mathcal{J}_L^s$, only information of $B_{\Delta\Delta}$ contributes. Consequently, we aim for a surrogate of the mappings

$$\boldsymbol{\xi}^r(\omega) \mapsto B_{\Delta\Delta}^s(\boldsymbol{\xi}^r(\omega)), \quad \forall (r,s) \in \mathcal{I}_{\text{active}}. \tag{41}$$

The surrogates of this mappings involve the largest coefficient matrices, depending only on the local dual degrees of freedom.

- We are now concerned with constructing surrogates to build $\tilde{S}_{\Pi\lambda}$. Note that with the notation in (40) it follows
$$A_{\Pi L}^s A_{LL}^{s^{-1}} \mathcal{J}_L^{s^T} = (A_{\Pi I}^s B_{I\Delta}^s + A_{\Pi\Delta}^s B_{\Delta\Delta}^s) \mathcal{J}_\Delta^{s^T}.$$
Thus, we aim for surrogates of the mapping
$$\boldsymbol{\xi}^s(\omega) \mapsto [A_{\Pi I}^s B_{I\Delta}^s + A_{\Pi\Delta}^s B_{\Delta\Delta}^s](\boldsymbol{\xi}^r(\omega)), \quad \forall (r,s) \in \mathcal{I}_{\text{active}}. \tag{42}$$
Coefficient matrices of the involved surrogates only depend on the number of local primal d.o.f.s times local dual d.o.f.s and are thus rather small if the coarse space is small.
- The SCHUR complement matrix $\tilde{S}_{\Pi\Pi}$ is treated as in the parametric SCHUR complement method in Section 4.2.1 via surrogates of
$$\boldsymbol{\xi}^r(\omega) \mapsto S_{\Pi\Pi}^s(\boldsymbol{\xi}^r(\omega)), \quad \forall (r,s) \in \mathcal{I}_{\text{active}}, \tag{43}$$
whereas the coefficient matrix sizes only depend on local degrees of freedom associated to the coarse space and hence are rather small compared to the classic coarse space in the SCHUR complement method.

The right-hand side of the parametric system can also be computed via surrogates.

- The local surrogates employed for the evaluation of $\tilde{b}(\boldsymbol{\xi}(\omega))$ are given by
$$\boldsymbol{\xi}^r \mapsto b_\Pi^s(\boldsymbol{\xi}^r(\omega)) := f_\Pi^s - A_{\Pi L}^s(\boldsymbol{\xi}^r(\omega)) A_{LL}^s(\boldsymbol{\xi}^r(\omega))^{-1} f_L^s, \tag{44}$$
for all active indices (s,r).
- The computation of $\tilde{b}_\lambda$ can be based on local surrogates
$$\boldsymbol{\xi}^r(\omega) \mapsto B_{\Delta I}^s(\boldsymbol{\xi}^r(\omega)) f_I^s + B_{\Delta\Delta}^s(\boldsymbol{\xi}^r(\omega)) f_\Delta^s, \tag{45}$$
for active indices (s,r) in addition to the surrogates for $\tilde{S}_{\Pi\lambda}$, $\tilde{S}_{\Pi\Pi}$ and $\tilde{b}$.

Note that all local surrogates can be computed in parallel and stored separately. The suggested approach is summarized in Algorithm 4.

Algorithm 4 Realization in parametric FETI-DP

Input: ○sample $\mathbf{y}_k := \boldsymbol{\xi}_k(\omega) = [\boldsymbol{\xi}_k^1, \ldots, \boldsymbol{\xi}_k^M](\omega)$
○ local based system surrogates for $\boldsymbol{\xi}(\omega) \mapsto [F, \tilde{S}_{\Pi\Pi}, \tilde{S}_{\Pi\lambda}](\boldsymbol{\xi}(\omega))$
○ local based surrogates for preconditioner of (parametric) F.

Output: approximated realization of $u_k = u(\boldsymbol{\xi}_k(\omega))$ or subdomain parts $u_k^s = u_{k|D_s}$.

1: Compute r.h.s. sample $\tilde{b}_k = [f_L, \tilde{b}_{\Pi,k}, \tilde{b}_{\lambda,k}] = \tilde{b}(\boldsymbol{\xi}_k(\omega))$ (39) via surrogates (42)-(45).
2: Iteratively solve $F_k \lambda_k = \tilde{b}_{\lambda,k}$ via a preconditioned CG method via application of F_k and its preconditioner based on (41)-(43) and (51).
3: Solve SCHUR complement system $\tilde{S}_{\Pi\Pi,k} \tilde{u}_{\Pi,k} = \tilde{b}_{\Pi,k} + \tilde{S}_{\Pi\lambda,k} \lambda_k$ via (43).
4: Solve block diagonal system $A_{LL,k} u_{L,k} = f_L - \tilde{A}_{L\Pi,k} \tilde{u}_{\Pi,k} - \mathcal{J}_L^T \lambda_k$ in parallel.

The advantage of deterministic FETI-DP lies in its potential to lead to a *weakly scalable* algorithm that is enabled by a suitable choice of coarse space (associated with Π) and preconditioner P for the submatrix F [46]. In the context of domain decomposition techniques, the term *scalability* is associated

with the iterative solution cost of the discrete system, which should not deteriorate when the number of subdomains grows. Let H denote the diameter of the subdomain and h the maximal diameter of the subdomain mesh cells. It can then be shown that

$$\kappa(P^{-1}F) \leq C\left(1+\log\left(\frac{H}{h}\right)\right)^2, \tag{46}$$

where κ denotes the condition number, see *e.g.* [46] and the references therein. The construction of the scaled *lumped* and DIRICHLET preconditioner and its extension to the random case using surrogates is discussed in the Section 4.2.3.

4.2.3. *Preconditioner.* In what follows we introduce surrogates for two classic FETI-DP preconditioners, namely the *lumped* and the *Dirichlet* preconditioner P^{-1}_{lumped} and P^{-1}_{Dir}. These are given pointwise by

$$P^{-1}_{\#}(\boldsymbol{\xi}(\omega)) = \sum_{s=1}^{N_{\text{SD}}} W^s \mathcal{J}^s_\Delta M^s_\# \mathcal{J}^{s\,T}_\Delta W^s, \quad \# \in \{\text{lump, Dir}\}, \tag{47}$$

with $M_{\text{lump}} = A^s_{\Delta\Delta}$ and $M_{\text{Dir}} = A^s_{\Delta\Delta} - A^s_{\Delta I}A^{s\,-1}_{II}A^s_{I\Delta}$. Here, $M^s_\# = M^s_\#(\boldsymbol{\xi}^r(\omega))$ for all $(r,s) \in \mathcal{I}_{\text{active}}$. The diagonal scaling weight mappings W^s have a more involved parametric structure due to the coupling of neighboured random dependencies shown in (48).

We fix a subdomain D_s and let $D_{s'}$ be any neighboring subdomain such that there exist dual d.o.f.s Δ^s_i and $\Delta^{s'}_j$ in the local spaces associated with local meshes on those subdomains that both account for the same global dual deegree of freedom. We collect those $D_{s'}$ into D^s_Δ, noting that $D_s \in D^s_\Delta$ per definition. Then, following [41], the diagonal scaling W^s is defined as

$$(W^s)_{ii} = \operatorname{diag}(A^s_{\Delta\Delta})_{ii}\left(\sum_{s':D_{s'}\in D^s_\Delta} \operatorname{diag}(A^{s'}_{\Delta\Delta})_{jj}\right)^{-1}. \tag{48}$$

With this construction, the diagonal scaling enables the preconditioner to take material heterogeneities into account. An important observation is that if the assembled local dual matrices $A^s_{\Delta\Delta}$ and their neighborhood counterparts $A^{s'}_{\Delta\Delta}$ depend on $\boldsymbol{\xi}^r$ and $\boldsymbol{\xi}^{r'}$, respectively, then W^s is a matrix valued function depending on $\boldsymbol{\xi}^r$ and $\boldsymbol{\xi}^{r'}$. Hence, a direct surrogate construction may be not applicable due to the sum of involved local parameter dimensions.

Since the underlying physical local meshes are fixed, we can work around this issue. For s' such that $D_{s'} \in D^s_\Delta$, we introduce diagonal matrices $W^s_{s'}$ with

$$(W^s_{s'})_{ii} = \begin{cases} \operatorname{diag}(A^{s'}_{\Delta\Delta})_{jj} & \exists j : \Delta^{s'}_j, \Delta^s_i \text{ share common global dual d.o.f.} \\ 0, & \text{else.} \end{cases} \tag{49}$$

Then, we can compactly write

$$W^s = \operatorname{diag}(A^s_{\Delta\Delta})\left(\sum_{s':D_{s'}\in D^s_\Delta} W^s_{s'}\right)^{-1}, \tag{50}$$

where $W^s_{s'} = W^s_{s'}(\boldsymbol{\xi}^{r'})$ for all $(r',s') \in \mathcal{I}_{\text{active}}$. With this construction, we may generate surrogate of the following maps, which depend only on local parameters,

$$\boldsymbol{\xi}^r(\omega) \mapsto \begin{cases} M^s_\#(\boldsymbol{\xi}^r(\omega)), & \# \in \{\text{lump, Dir}\} \\ \operatorname{diag}(A^s_{\Delta\Delta}(\boldsymbol{\xi}^r(\omega))), & \\ W^s_{s'}(\boldsymbol{\xi}^r(\omega)), & D_{s'} \in D^s_\Delta, \end{cases} \quad \forall (r,s) \in \mathcal{I}_{\text{active}}, \tag{51}$$

and define the application of the preconditioner based on these local surrogates.

Remark 4.5. *If the aim of the computation involves the recovering of approximate sample solutions over the whole domain, then A^s_{LL} needs to be inverted per sample separately, see Algorithm 4. In this case, for each s, A^s_{LL} is assembled sample-wise such that $A^s_{\Delta\Delta}$ is accessible. Then, we propose to only build a surrogate for $\boldsymbol{\xi}^r(\omega) \mapsto M^s_{\mathit{Dir}}(\boldsymbol{\xi}^r(\omega))$ for $(r,s) \in \mathcal{I}_{\mathit{active}}$ as this map would introduce several inversions of $A^{s^{-1}}_{II}$ in the solution iteration scheme of a preconditioned conjugate gradient method.*

Remark 4.6. *In summary, we presented a pointwise surrogate approach, which for each sample up to surrogate precision enables weak-scalability based on the deterministic results. Alternatively, a fixed preconditioner such as the mean $\mathbb{E}[P^{-1}_{\#}]$ can be considered as in* [11] *for the* SCHUR *complement method.*

4.2.4. *Parametric FETI-DP for cluster sampling.* In this subsection we consider cluster sampling (as a special case) that corresponds to a piecewise constant approximation of the involved parametric assembled discretization in the spirit of zero order gHPCE from Section 3.2. While the discretization is applicable to low local parametric dimensions only due to cost aspects, it turns out that the resulting surrogates have a very simple structure. In this case, the surrogates are not needed to be build explicitly and the method involving its preconditioner is a simple generalization of the classic deterministic FETI-DP in all its algorithmic details, like the use of precomputed LU decompositions of the involved inverse matrix applications. We shall describe the benefits illustrated with the random FETI-DP matrix F.

Let (r,s) be active and consider the zero order gHPCE for any involved local random matrix M^s such that

$$M^s(\boldsymbol{\xi}^r(\omega)) \approx M^s_{\mathbf{0}}(\boldsymbol{\xi}^r(\omega)) := \sum_{j\in\mathcal{J}} M^s_j \Psi_{\mathbf{0},j}(\boldsymbol{\xi}^r(\omega)). \tag{52}$$

A key observation follows if M^s_j is invertible for all $j \in \mathcal{J}$. By the push-forward $\mu^r = \mathbb{P}_{\#\boldsymbol{\xi}^r}$ and identification $\mathbf{y}^r = \boldsymbol{\xi}^r(\omega)$ and $\Xi^r = \cup_{j\in\mathcal{J}}\Xi^r_j$, it holds pointwise

$$M^s(\boldsymbol{y}^r)^{-1} = \left(M^s_{j'}\Psi_{\mathbf{0},j'}(\boldsymbol{y}^r)\right)^{-1}, \quad \mu^r\text{-a.e., } \boldsymbol{y}^r \in \Xi^r_{j'}. \tag{53}$$

As a consequence, *e.g.* the inverse of the SCHUR complement structure $S^s_{\Pi\Pi}(\boldsymbol{\xi}^r(\omega))^{-1}$ has an easy form given as

$$S^s_{\Pi\Pi}(\boldsymbol{\xi}^r(\omega)) = \sum_{j\in\mathcal{J}} S^s_{\Pi\Pi j}\Psi_{\mathbf{0},j}(\boldsymbol{\xi}^r(\omega)), \tag{54}$$

where only one summand contributes to a realization of $\boldsymbol{\xi}^r$. With that structure, for the s-th summand $R^s_\Pi A^s_{\Pi L} A^{s^{-1}}_{LL} \mathcal{J}^{sT}_L$ in the definition of $\tilde{S}_{\Pi\lambda}$, it follows that

$$[A^s_{\Pi L}A^{s^{-1}}_{LL}](\boldsymbol{y}^r) = \left(\sum_{j\in\mathcal{J}} A^s_{\Pi L j}\Psi_{\mathbf{0},j}(\boldsymbol{y}^r)\right)\left(\sum_{j'\in\mathcal{J}}\left(A^s_{LLj'}\Psi_{\mathbf{0},j'}(\boldsymbol{y}^r)\right)^{-1}\right) \tag{55}$$

$$= \sum_{j\in\mathcal{J}} A^s_{\Pi L j}\left(A^s_{LLj}\right)^{-1}\chi_{\Gamma^r_j}(\boldsymbol{y}^r), \tag{56}$$

with indicator function $\chi_{\Gamma^r_j}$. Thus, for a global realization, the application of F relies on precomputed factorizations of A^s_{LLj} and storage of all involved coefficient matrices for $s = 1,\dots,N_{\mathsf{SD}}$, and $j \in J$. This indicates a limiting factor if $|J|$ gets too large by the *curve of dimensionality*.

The piecewise constant approximation scheme in the stochastic space is suiteable for domain-wise random fields $\omega \mapsto a(x,\omega) = a(x, X(\omega))$ parametrized by a discrete random variable X with finite

dimensional image $\{x_1, \dots, x_{|J|}\}$. Such fields might be represented as

$$a(x, X(\omega)) = \varphi_0(x) + \sum_{j \in J} \pi_j(X(\omega))\varphi_j(x), \tag{57}$$

with polynomials π_j with $\pi_j(x_i) = \delta_{ij}$ and functions φ_j in physical space. A special case of this is the *checkerboard material* with $\pi_0(y) = y$, $\pi_1(y) = 1 - y$, and $\varphi_j \equiv j$.

5. Numerical Experiments

In order to illustrate the performance of the proposed partition of unity interpolation approach of Section 3.3, we discuss some numerical examples. The implementation of the hybrid domain decomposition method for random domains was carried out as part of the open source `ALEA` library [14] with the deterministic FE backend `FEniCS` [21] for the assembly of local matrices. The discrete random coordinate spaces are realized with a custom implementation of a hierachical tree based decomposition of M-dimensional cells such as tensorized hyper quadrilaterals. Each such element can be refined anisotropically by bisection separately in each coordinate direction. Additionally, a cell is refined into *macro-elements* (marked as gray in the figures below) while remaining a hyper quadrilateral if sub-areas are not necessary for further refinement in the marking process.

Two experiments based on the model problem (1) are considered with homogeneous Dirichlet boundary conditions. In Section 5.1, we examine a smooth local parametric dependence with an additional challenge introduced by a non-linear coupling of random and physical coordinates. A random cookie problem as described in Example 2.9 representing non-smooth data is presented in Section 5.2.

Figures 3-5 (respectively 9-11) illustrate the adaptive surrogate generation. The figures from top to buttom show: the partitioned parametric domain Γ^s, employed polynomial degrees (4: blue, 3: yellow, 2 orange), trust/no-trust zones and local errors.

5.1. **Smooth problem with non-linear coupling.** We consider $D = [0,1]^2$ and a partition of D into $N \times N$ subsquares D_s with $N = 3$, $x = (x_1, x_2)$. A smooth random field with a coupling of physical and stochastic coordinates is given by

$$a(x, \boldsymbol{\xi}) = a(x, \boldsymbol{\xi}^s(\omega)) = 1.1 + \sin(\alpha\pi(x_1\xi_1(\omega) + x_2\xi_2(\omega))), \quad x \in D_s, \tag{58}$$

with $\boldsymbol{\xi}^s = (\xi_1^s, \xi_2^s)$, $\alpha = 0.7$ and independent $\xi_i^s \sim \mathcal{U}[-1,1]$, for $i = 1, M = 2$, $s = 1, \dots, N_{\mathsf{SD}} = 9$, resulting in a total of 18 random dimensions. In Figures 3-5, we illustrate the adaptive partitioning process of a local random image space $[-1,1]^M$ based on Algorithm 1. In the experiment we utilize a physical discretisation with $p = 1$ FE on uniform 30×30 triangulations of D_s, $s = 1, \dots, N_{\mathsf{SD}}$. The non-linear coupling of random and physical coordinates introduces a layer of the involved matrix valued random maps that differs for all $s = 1, \dots, 9$, also depending on the size of values taken in x. We illustrate the different structures in Figure 6 by final meshes obtained by the adaptive scheme. We point out that $\alpha = 2\pi$, or on larger domains D and thus related larger range of x, the surrogate construction becomes more involved and finer layers have to be resolved. In the numerical investigation, it is observed that given a $\mathrm{tol} > 0$ for the local interface surrogates, the error between a sampled solution based on surrogates denoted by $\hat{u}_h^k$ and its analogue (Monte Carlo) sample solution denoted by u_h^k is of higher order. The situation is illustrated in Figure 7 with a pointwise difference of order $\mathcal{O}(10^{-6})$ and $\|\hat{u}_h^k - u_h^k\|_{H_0^1(D)} / \|u_h^k\| \in \mathcal{O}(6 \times 10^{-5})$.

5.2. **Cookie problem, model problem for more general composite materials.** We consider a rectangular domain $D = [0, W] \times [0, H]$ with parameters $H, W > 0$ such that D can be decomposed

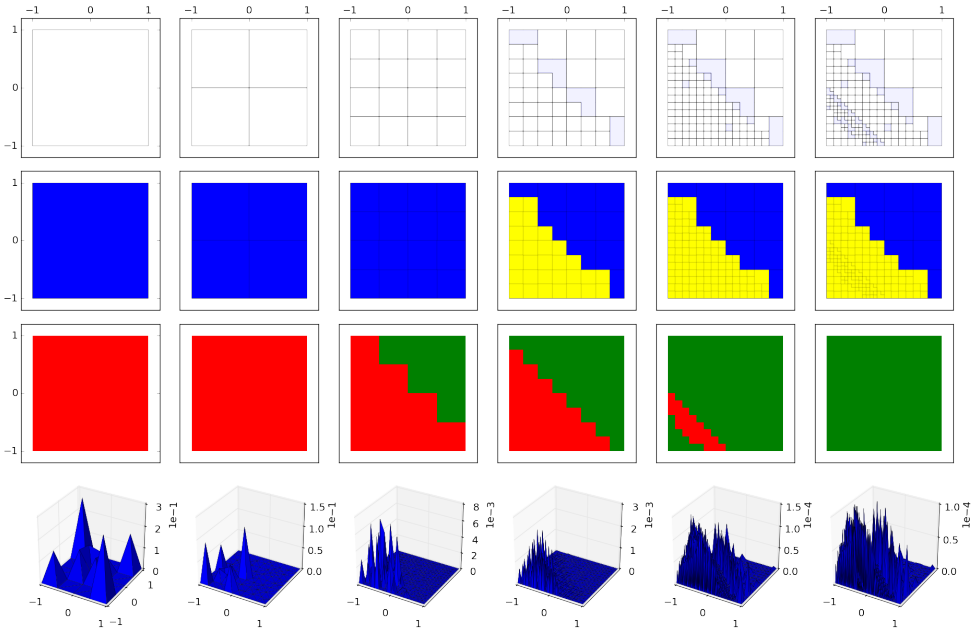

FIGURE 3. Adaptive surrogate construction based on macro-element anisotropic refinement procedure for $\boldsymbol{\xi}^s \mapsto B^s_{\Delta\Delta}(\boldsymbol{\xi}^s)$ associated to an inner square D_s with $\mathrm{tol} = 10^{-4}$ and 100% trusted zone after 6 iterations.

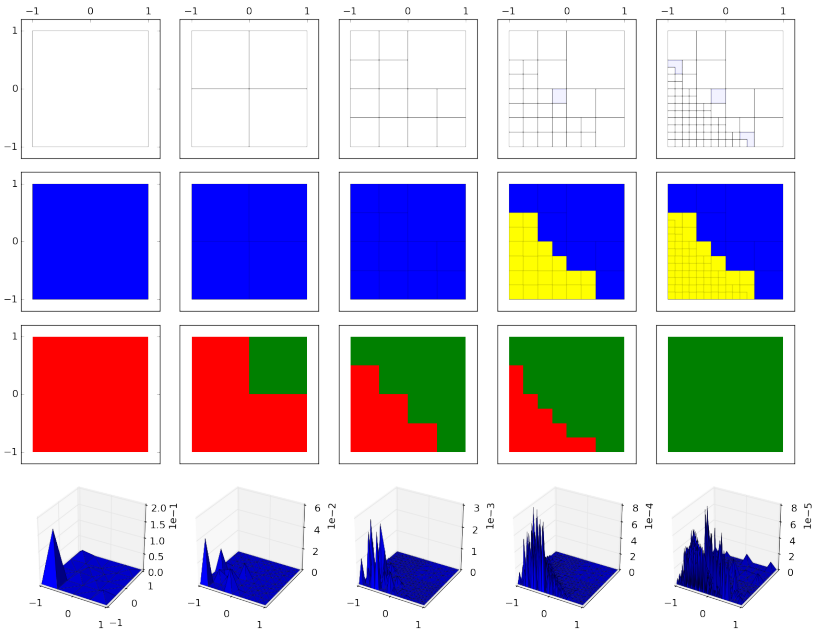

FIGURE 4. Adaptive surrogate construction procedure for $\boldsymbol{\xi}^s \mapsto S^s_{\Pi\lambda}(\boldsymbol{\xi}^s)$ associated to an inner square D_s with $\mathrm{tol} = 10^{-4}$ and 100% trusted zone after 5 iterations.

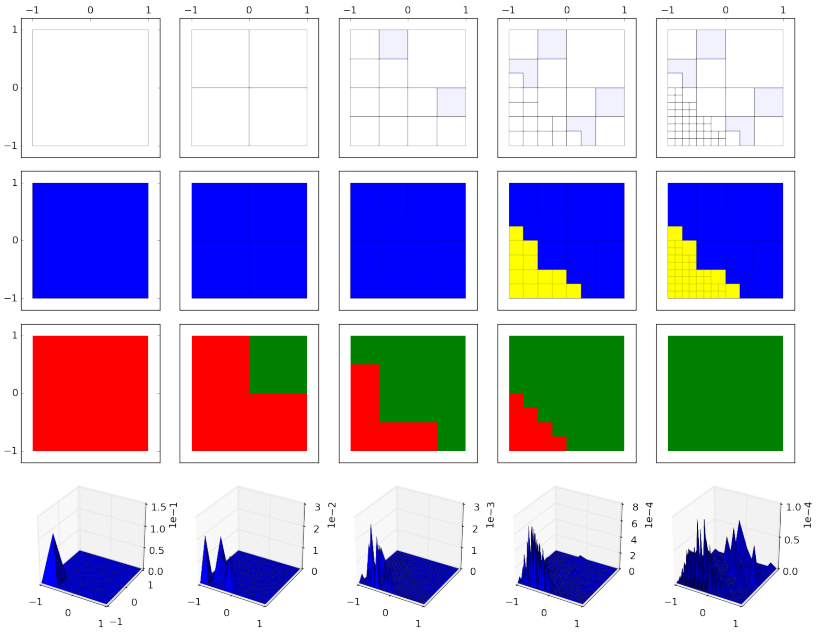

FIGURE 5. Adaptive surrogate construction procedure for $\boldsymbol{\xi}^s \mapsto S^s_{PP}(\boldsymbol{\xi}^s)$ associated to an inner square D_s with $\mathrm{tol} = 10^{-4}$ and 100% trusted zone after 5 iterations.

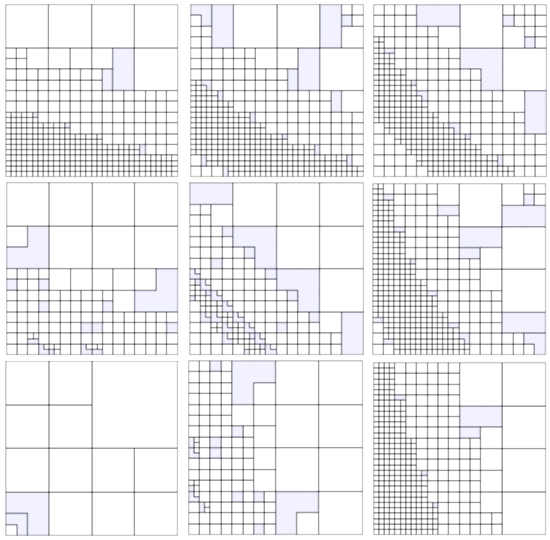

FIGURE 6. Final meshes on the surrogate random domain $\operatorname{img} \boldsymbol{\xi}^s = [-1,1]^2$ for $s = 1, \dots, 9$ with $\mathrm{tol} = 10^{-4}$ and resulting 100% trusted region for the maps $\boldsymbol{\xi}^s \mapsto B^s_{\Delta\Delta}(\boldsymbol{\xi}^s)$ using macro-elements (gray) and an anisotropic refinement. The polynomial degrees vary from 2 for very small to 4 for larger elements.

into squares D_s for $s = 1, \dots, N_{\mathsf{SD}} = N_H N_W$, where N_H (respectively N_W) denotes the number of squares in their respective direction.

Remark 5.1. *For the physical discretization, a fixed uniform (local) triangular mesh is used implicitly for each realization of the composite structure. In particular, given a realization of the composite, the*

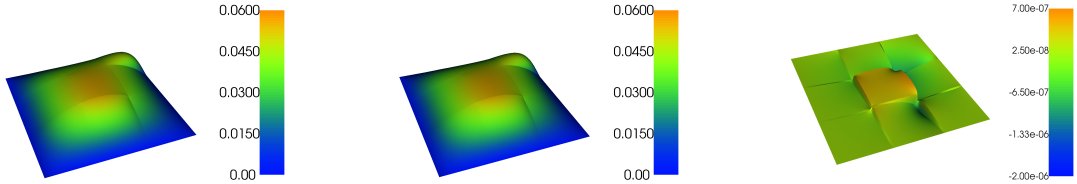

FIGURE 7. From left to right: MC sample, surrogate based sample and difference of globally reconstructed discrete solution for the problem in Section 5.1, using a uniform 30×30 triangular mesh on each of the 3×3 subdomains.

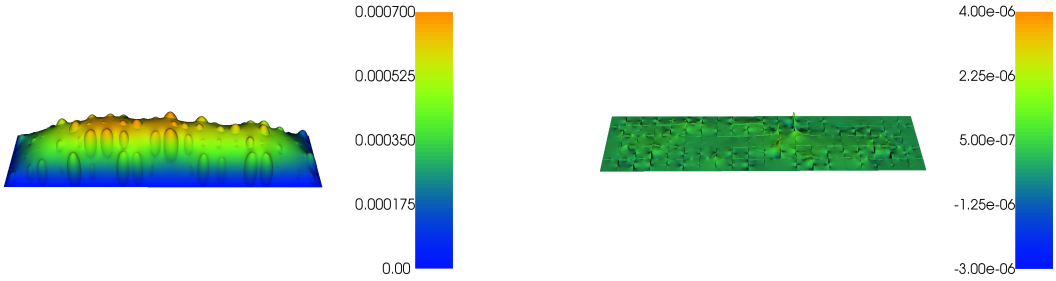

FIGURE 8. Left: Surrogate based sample $\hat{u}_h^k$ for the random cookie problem on 20×5 subdomains using $p = 1$ FE on local uniform 40×40 triangular meshes on D_s. Right: Pointwise difference to MC sampled discrete solution u_h^k. Local surrogates build with tol $= 10^{-2}$ leading to relative $H_0^1(D)$ errors of $\|\hat{u}_h^k - u_h^k\|_{H_0^1(D)}/\|u_h^k\| \in \mathcal{O}(9 \times 10^{-3})$.

mesh does not resolve the jump in the coefficient, which in a deterministic setting is critical from an accuracy point of view. In order to benefit from using such a fixed mesh, the FE basis functions can be enriched by an element-wise basis function with a jump in the gradient of the discrete basis function as described in [28]*. With this, the presented technique exhibits a better approximation quality with respect to the solution* u*.*

On each square domain D_s, the random field $A = aI$ $\mathbb{P}$-a.e. is described by

$$a(x,\omega) = a(x, \boldsymbol{\xi}^s(\omega)) = \chi_{B(\boldsymbol{\xi}^s(\omega))}(x) + 20(1 - \chi_{B(\boldsymbol{\xi}^s(\omega))}(x)), \quad x \in D_s. \tag{59}$$

Here, $B^s(\boldsymbol{\xi}^s(\omega))$ denotes a random ball modelled by a random radius ϱ and a random x-position $p^s_{x_1}$ of a point $\boldsymbol{p}^s = (p^s_{x_1}, p^s_{x_2})$ in D_s s.t. $(\varrho, p^s_x) = \varphi^s(\xi^s_1(\omega), \xi^s_2(\omega))$ with a map φ^s choosen such that $B(\boldsymbol{\xi}^s(\omega))$ is uniformly bounded away from ∂D_s by a given distance as in Example 2.9. By a push-forward we may identify $\boldsymbol{y}^s = \boldsymbol{\xi}^s(\omega)$ and interpret $\boldsymbol{y}^s \mapsto a(\cdot, \boldsymbol{y}^s)$ as an element in $L^2([-1,1]^2; L^\infty(D))$. We stress that $a \notin \mathcal{C}([-1,1]^2; L^\infty(D))$ but $a \in L^\infty([-1,1]^2; L^\infty(D))$. The defined composite material coefficient lacks regularity in the random as well as the physical coordinates, satisfying the conditions of section 2. Note that the full random dimension is $M' = 2N_H N_W$, *e.g.* with $M' = 200$ for 20×5 squares as illustrated in Figure 8. Due to the same structure of the domain-wise non-periodic material description for the homogeneous DIRICHLET problem, it suffices to compute local surrogates for 9 subdomains only (4 associated to each corner and edge, 1 inner domain. The adaptive procedure is illustrated for the inner domain case in Figures 9-11.

We point out the refinement pattern towards the boundary of the parameter domain. The right interface corresponds to the case of maximal radius ϱ of the random ball, the top and bottom interface

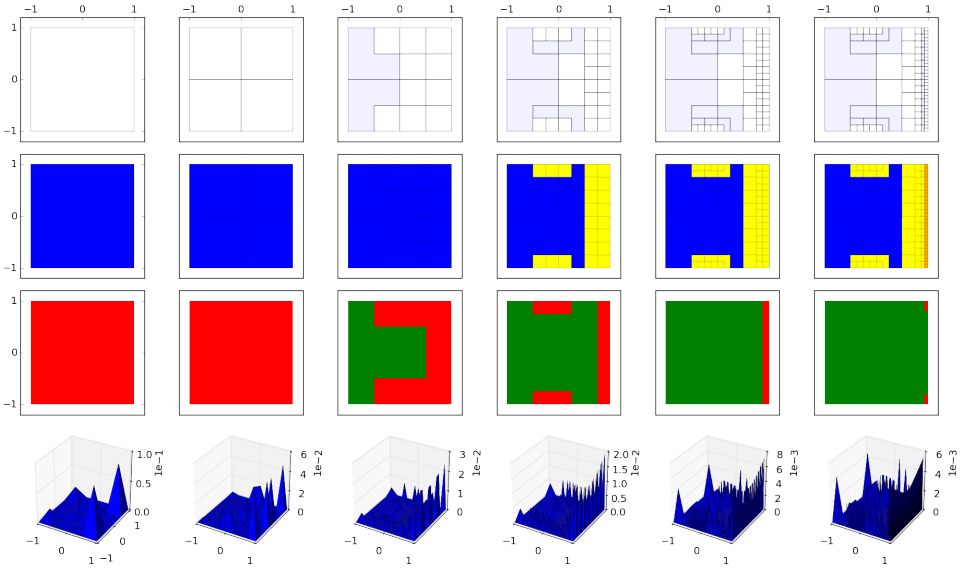

FIGURE 9. Adaptive surrogate construction based on macro-element anisotropic refinement procedure for $\boldsymbol{\xi}^s \mapsto B^s_{\Delta\Delta}(\boldsymbol{\xi}^s)$ for a inner square D_s with $\mathrm{tol} = 0.5 \times 10^{-2}$. 99.41% trusted zone after 6 iterations.

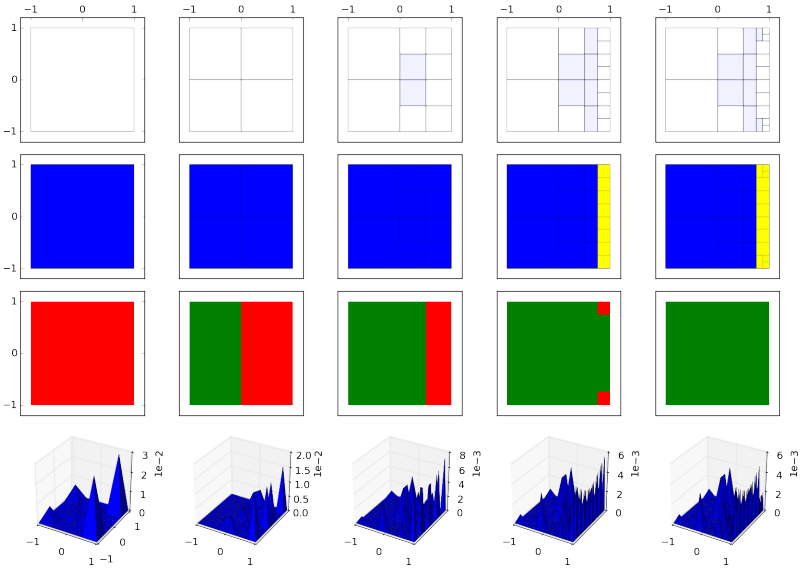

FIGURE 10. Adaptive surrogate construction procedure for $\boldsymbol{\xi}^s \mapsto S^s_{\Pi\lambda}(\boldsymbol{\xi}^s)$ for a inner square D_s with $\mathrm{tol} = 0.5 \times 10^{-2}$. 100% trusted zone after 5 iterations.

correspond to the maximal displacement of the ball. Due to the surrogate construction based on a semi-discretization, given sufficiently fine physical meshes, the intersection of the random ball and the support of the basis functions associated locally to the boundary shrinks. Thus, the dependence of the non-smooth influence gets smaller. Furthermore, we observe a constant error for $B_{\Delta\Delta}$ in Figure

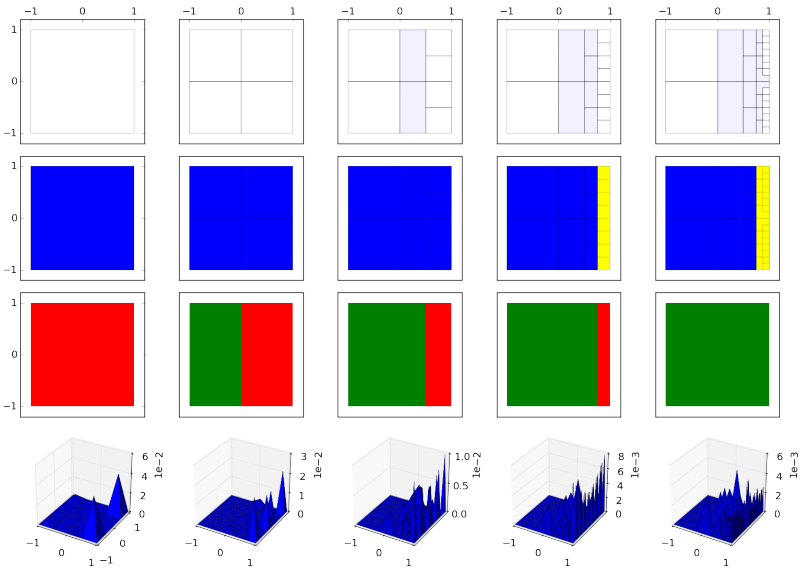

FIGURE 11. Adaptive surrogate construction procedure for $\boldsymbol{\xi}^s \mapsto S^s_{PP}(\boldsymbol{\xi}^s)$ for a inner square D_s with $\mathrm{tol} = 0.5 \times 10^{-2}$. 100% trusted zone after 5 iterations.

9 that accounts for the remaining support interaction and exhibits a noteable very slow decrease. This interaction is further illustrated in Figure 12, when solving for a smaller tolerance $\mathrm{tol} = 10^{-3}$.

In the numerical experiments, building the surrogate $\boldsymbol{\xi}^s \mapsto A^s_{LL}(\boldsymbol{\xi}^s)^{-1}$ as in Remark 3.8 leads to massive uniform refinements with an (arbitrarily) slow error decrease. However, the involved interface operators are observed to exhibit rather smooth sub-areas in the parametric space with remaining small non-trusted areas.

ACKNOWLEDGEMENTS

The authors gladly acknowledge the funding of RG in the DFG SPP 1886 “Polymorphic uncertainty modelling for the numerical design of structures”.
The authors would like to thank Prof. Hermann Matthies for pointing out Remark 2.10.

REFERENCES

[1] C. AMROUCHE, C. CONCA, A. GHOSH, AND T. GHOSH, *Uniform $W^{1,p}$ estimate for elliptic operator with robin boundary condition in $\mathcal{C}^1$ domain*, arXiv preprint arXiv:1805.09519, (2018).

[2] I. BABUŠKA AND P. CHATZIPANTELIDIS, *On solving elliptic stochastic partial differential equations*, Comput. Methods Appl. Mech. Engrg., 191 (2002), pp. 4093–4122, https://doi.org/10.1016/S0045-7825(02)00354-7, http://dx.doi.org/10.1016/S0045-7825(02)00354-7.

[3] I. BABUŠKA, R. TEMPONE, AND G. E. ZOURARIS, *Solving elliptic boundary value problems with uncertain coefficients by the finite element method: the stochastic formulation*, Comput. Methods Appl. Mech. Engrg., 194 (2005), pp. 1251–1294, https://doi.org/10.1016/j.cma.2004.02.026, http://dx.doi.org/10.1016/j.cma.2004.02.026.

[4] M. BACHMAYR, A. COHEN, AND W. DAHMEN, *Parametric pdes: sparse or low-rank approximations?*, IMA Journal of Numerical Analysis, 38 (2017), pp. 1661–1708.

[5] M. BACHMAYR, A. COHEN, AND G. MIGLIORATI, *Representations of gaussian random fields and approximation of elliptic pdes with lognormal coefficients*, Journal of Fourier Analysis and Applications, 24 (2018), pp. 621–649.

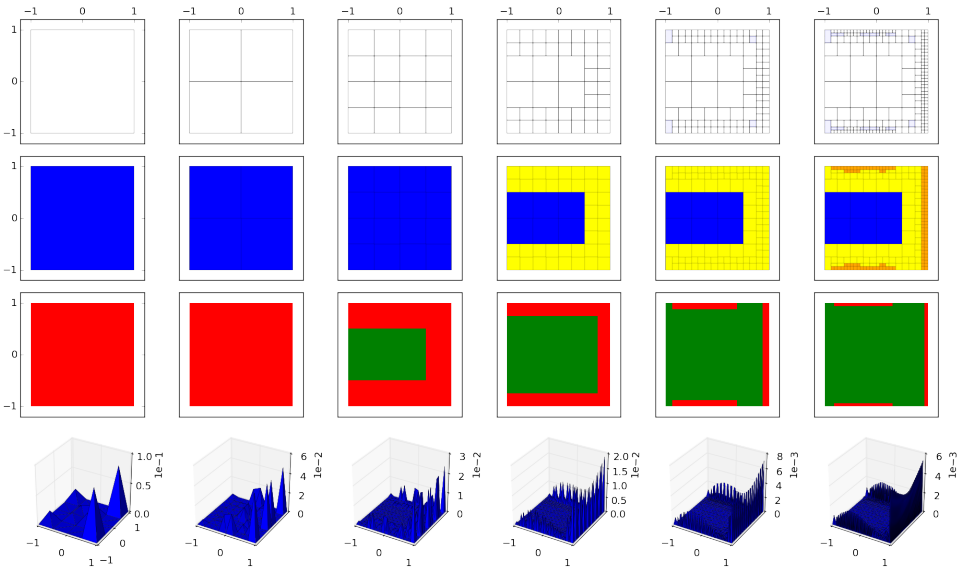

FIGURE 12. Adaptive procedure for $\boldsymbol{\xi}^s \mapsto B^s_{\Delta\Delta}(\boldsymbol{\xi}^s)$ associated to an inner domain D_s with $\mathrm{tol} = 10^{-3}$. The maximal displacement areas and the maximal radius areas dominate the error and remain non-trusted. After 6 iterations a trusted area of 93.35% is obtained.

[6] A. BARTH AND A. STEIN, *A study of elliptic partial differential equations with jump diffusion coefficients*, arXiv preprint arXiv:1712.04876, (2017).

[7] A. BONITO, R. A. DEVORE, AND R. H. NOCHETTO, *Adaptive finite element methods for elliptic problems with discontinuous coefficients*, SIAM Journal on Numerical Analysis, 51 (2013), pp. 3106–3134.

[8] M. CHEVREUIL, A. NOUY, AND E. SAFATLY, *A multiscale method with patch for the solution of stochastic partial differential equations with localized uncertainties*, Computer Methods in Applied Mechanics and Engineering, 255 (2013), pp. 255–274.

[9] K. A. CLIFFE, M. B. GILES, R. SCHEICHL, AND A. L. TECKENTRUP, *Multilevel monte carlo methods and applications to elliptic pdes with random coefficients*, Computing and Visualization in Science, 14 (2011), p. 3.

[10] A. A. CONTRERAS, P. MYCEK, O. LE MAITRE, F. RIZZI, B. DEBUSSCHERE, AND O. M. KNIO, *Parallel domain decomposition strategies for stochastic elliptic equations–part a: Local kl representations*, 2016.

[11] A. A. CONTRERAS, P. MYCEK, O. P. LE MAÎTRE, F. RIZZI, B. DEBUSSCHERE, AND O. M. KNIO, *Parallel domain decomposition strategies for stochastic elliptic equations part b: Accelerated monte carlo sampling with local pc expansions*, SIAM Journal on Scientific Computing, 40 (2018), pp. C547–C580.

[12] C. F. DUNKL AND Y. XU, *Orthogonal polynomials of several variables*, no. 155, Cambridge University Press, 2014.

[13] M. EIGEL, C. J. GITTELSON, C. SCHWAB, AND E. ZANDER, *Adaptive stochastic Galerkin FEM*, Comput. Methods Appl. Mech. Engrg., 270 (2014), pp. 247–269, https://doi.org/10.1016/j.cma.2013.11.015, http://dx.doi.org/10.1016/j.cma.2013.11.015.

[14] M. EIGEL, R. GRUHLKE, M. MARSCHALL, P. TRUNSCHKE, AND E. ZANDER, *Alea - a python framework for spectral methods and low-rank approximations in uncertainty quantification*, https://bitbucket.org/aleadev/alea.

[15] M. EIGEL, M. MARSCHALL, M. PFEFFER, AND R. SCHNEIDER, *Adaptive stochastic galerkin fem for lognormal coefficients in hierarchical tensor representations*, arXiv preprint arXiv:1811.00319, (2018).

[16] M. EIGEL AND C. MERDON, *Local equilibration error estimators for guaranteed error control in adaptive stochastic higher-order galerkin finite element methods*, SIAM/ASA Journal on Uncertainty Quantification, 4 (2016), pp. 1372–1397.

[17] M. EIGEL, M. PFEFFER, AND R. SCHNEIDER, *Adaptive stochastic Galerkin FEM with hierarchical tensor representations*, Numerische Mathematik, 136 (2017), pp. 765–803, https://doi.org/10.1007/s00211-016-0850-x, https://doi.org/10.1007/s00211-016-0850-x.

[18] M. EIGEL, R. SCHNEIDER, P. TRUNSCHKE, AND S. WOLF, *Variational monte carlo-bridging concepts of machine learning and high dimensional partial differential equations*, arXiv preprint arXiv:1810.01348, (2018).

[19] O. G. ERNST, A. MUGLER, H.-J. STARKLOFF, AND E. ULLMANN, *On the convergence of generalized polynomial chaos expansions*, ESAIM: Mathematical Modelling and Numerical Analysis, 46 (2012), pp. 317–339.

[20] C. FARHAT, M. LESOINNE, P. LETALLEC, K. PIERSON, AND D. RIXEN, *Feti-dp: a dual–primal unified feti methodâĂŤpart i: A faster alternative to the two-level feti method*, International journal for numerical methods in engineering, 50 (2001), pp. 1523–1544.

[21] *FEniCS Project - Automated solution of Differential Equations by the Finite Element Method*, http://fenicsproject.org.

[22] L. GRASEDYCK, D. KRESSNER, AND C. TOBLER, *A literature survey of low-rank tensor approximation techniques*, GAMM-Mitteilungen, 36 (2013), pp. 53–78.

[23] M. GRIEBEL, *Adaptive sparse grid multilevel methods for elliptic pdes based on finite differences*, Computing, 61 (1998), pp. 151–179.

[24] K. GRÖGER, *A $W^{1,p}$-estimate for solutions to mixed boundary value problems for second order elliptic differential equations*, Mathematische Annalen, 283 (1989), pp. 679–687.

[25] R. GRUHLKE, M. EIGEL, D. HÖMBERG, M. DRIESCHNER, AND Y. PETRYNA, *A hybrid stochastic domain decomposition method for partial differential equations with localised possibly rough random data*, PAMM, 18 (2018), p. e201800434, https://doi.org/10.1002/pamm.201800434, https://onlinelibrary.wiley.com/doi/abs/10.1002/pamm.201800434, https://arxiv.org/abs/https://onlinelibrary.wiley.com/doi/pdf/10.1002/pamm.201800434.

[26] W. HACKBUSCH, *Tensor spaces and numerical tensor calculus*, vol. 42, Springer Science & Business Media, 2012.

[27] M. HADIGOL, A. DOOSTAN, H. G. MATTHIES, AND R. NIEKAMP, *Partitioned treatment of uncertainty in coupled domain problems: A separated representation approach*, Computer Methods in Applied Mechanics and Engineering, 274 (2014), pp. 103–124.

[28] A. IBRAHIMBEGOVIC, *Nonlinear solid mechanics: theoretical formulations and finite element solution methods*, vol. 160, Springer Science & Business Media, 2009.

[29] D. J.-C. KENIG, *The inhomogeneous dirichlet problem in lipschitz domains*, J. funct. Anal, 130 (1995), pp. 161–219.

[30] A. KLAWONN, P. RADTKE, AND O. RHEINBACH, *Feti-dp methods with an adaptive coarse space*, SIAM Journal on Numerical Analysis, 53 (2015), pp. 297–320.

[31] A. KLAWONN, O. RHEINBACH, AND O. B. WIDLUND, *An analysis of a feti–dp algorithm on irregular subdomains in the plane*, SIAM Journal on Numerical Analysis, 46 (2008), pp. 2484–2504.

[32] A. KLAWONN AND O. B. WIDLUND, *Dual-primal feti methods for linear elasticity*, Communications on Pure and Applied Mathematics: A Journal Issued by the Courant Institute of Mathematical Sciences, 59 (2006), pp. 1523–1572.

[33] M. J. KÜHN, *Adaptive FETI-DP and BDDC methods for highly heterogeneous elliptic finite element problems in three dimensions*, PhD thesis, Universität zu Köln, 2018.

[34] F. Y. KUO AND D. NUYENS, *Application of quasi-monte carlo methods to elliptic pdes with random diffusion coefficients: a survey of analysis and implementation*, Foundations of Computational Mathematics, 16 (2016), pp. 1631–1696.

[35] J. MANDEL AND B. SOUSEDÍK, *Bddc and feti-dp under minimalist assumptions*, Computing, 81 (2007), pp. 269–280.

[36] N. G. MEYERS, *An l^p-estimate for the gradient of solutions of second order elliptic divergence equations*, Annali della Scuola Normale Superiore di Pisa-Classe di Scienze, 17 (1963), pp. 189–206.

[37] L. MU AND G. ZHANG, *A Domain-Decomposition Model Reduction Method for Linear Convection- Diffusion Equations with Random Coefficients*, arXiv e-prints, (2018), arXiv:1802.04187, p. arXiv:1802.04187, https://arxiv.org/abs/1802.04187.

[38] F. NOBILE, R. TEMPONE, AND C. G. WEBSTER, *A sparse grid stochastic collocation method for partial differential equations with random input data*, SIAM Journal on Numerical Analysis, 46 (2008), pp. 2309–2345.

[39] S. RAHMAN, *Wiener–hermite polynomial expansion for multivariate gaussian probability measures*, Journal of Mathematical Analysis and Applications, 454 (2017), pp. 303–334.

[40] O. RHEINBACH, *Parallel scalable iterative substructuring: Robust exact and inexact feti-dp methods with applications to elasticity [phd thesis]*, Essen (Germany): University of Duisburg-Essen, Essen, (2006).

[41] D. J. RIXEN AND C. FARHAT, *A simple and efficient extension of a class of substructure based preconditioners to heterogeneous structural mechanics problems*, International Journal for Numerical Methods in Engineering, 44 (1999), pp. 489–516.

[42] C. SCHWAB, *P-and Hp-Finite Element Methods: Theory and Applications in Solid and Fluid Mechanics (Numerical Mathematics and Scientific Computation)*, Oxford University Press, New York, 1999.

[43] W. SUBBER AND A. SARKAR, *Dual-primal domain decomposition method for uncertainty quantification*, Computer Methods in Applied Mechanics and Engineering, 266 (2013), pp. 112–124.

[44] L. TARTAR, *An introduction to Sobolev spaces and interpolation spaces*, vol. 3, Springer Science & Business Media, 2007.
[45] A. L. TECKENTRUP, R. SCHEICHL, M. B. GILES, AND E. ULLMANN, *Further analysis of multilevel monte carlo methods for elliptic pdes with random coefficients*, Numerische Mathematik, 125 (2013), pp. 569–600.
[46] A. TOSELLI AND O. WIDLUND, *Domain decomposition methods-algorithms and theory*, vol. 34, Springer Science & Business Media, 2006.
[47] H. TRIEBEL, *Theory of function spaces ii*, Bull. Amer. Math. Soc, 31 (1994), pp. 119–125.
[48] X. WAN AND G. E. KARNIADAKIS, *An adaptive multi-element generalized polynomial chaos method for stochastic differential equations*, Journal of Computational Physics, 209 (2005), pp. 617–642.
[49] D. XIU AND G. E. KARNIADAKIS, *The wiener–askey polynomial chaos for stochastic differential equations*, SIAM journal on scientific computing, 24 (2002), pp. 619–644.